living. There are numerous, well-known conditions that can influence upper-extremity function, such as postoperative C5 palsy [5, 6] and late neurological deterioration [4]. Because upper-extremity function is more subtle and complicated than that of the lower extremity, a more detailed measure is essential for evaluation. However, there are few quantitative measures for total evaluation; the JOA score and its subscores are expressed as discrete variables, and the visual analog scale (VAS) can evaluate sensory function only.

The Disability of the Arm, Shoulder, and Hand (DASH) questionnaire was devised as a region-specific, patient-reported outcome measure to evaluate symptoms and functional status of the upper extremity, and the QuickDASH was developed as a shortened version [7, 8]. Many authors reported positive results of validity and responsiveness of DASH in patients with upper-extremity disorder [8, 9]. DASH and QuickDASH are appropriate for assessing disorders affecting upper-extremity functions, and symptoms can be assessed in a single, combined scale.

Although there are a few reports on the relationship between neck pain and DASH [10, 11], no report has documented the usefulness of DASH or QuickDASH for evaluating cervical myelopathy. We determined the efficacy of the QuickDASH questionnaire for evaluating functional outcomes of the upper extremity after cervical laminoplasty and compared the results with those of other commonly used assessment measures. To our knowledge, this is the first report on the usefulness of QuickDASH for cervical myelopathy.

Materials and methods

Study approval was given by the institutional review board of the Clinical Research Support Center of the University of Tokyo Hospital. Records of patients who underwent double-door laminoplasty for treatment of cervical laminoplasty between 1985 and 2008 and whose cases were followed at our department were retrospectively investigated. We mailed the questionnaires to the patients, and 608 patients who replied the questionnaires were included in the study. There were 351 patients who responded to all items. In addition, 139 were excluded by the following criteria; previous cervical spine surgery or other concomitant disease influencing symptoms and functional status of the upper extremity, including cerebral palsy, diabetic neuropathy, rheumatoid arthritis, or others. Of the 212 patients remaining, patients who had outpatient at the time of survey were included in this study.

Finally, 94 patients (59 men, 35 women) were enrolled. Average age at surgery was 62 (range 30–82) years, and mean follow-up was 61 (range 12–274) months. Diagnoses were cervical spondylosis in 57 patients, ossification of the posterior longitudinal ligament in 33, cervical disc herniation in nine, and ossification of yellow ligament in two.

The questionnaires included the QuickDASH Japanese version, Short-Form Health Survey of 36 questions (SF-36) [12, 13], Neck Disability Index (NDI) [14], and upper-extremity pain scale (Numerical Rating Scale 0–10). Patient satisfaction was also assessed by choosing either "satisfied,", "dissatisfied," or "neither."

QuickDASH consists of 11 items derived from DASH (Table 1). Each item has five response options ranging from "no difficulty or no symptom" to "unable to perform activity or very severe symptom," each scored on a scale of 1–5. These 11 items provide the QuickDASH score, which ranges from 0 (no disability) to 100 (the most severe disability) after summation of scores from all items and transformation [8].

The JOA score was used to evaluate preoperative and postoperative neurological functions at the time of survey (Table 2). The Hirabayashi method [15] was used to calculate the recovery rate of the JOA score according to the following formula: recovery rate (%) = (postoperative JOA score − preoperative JOA score) × 100/(17 − preoperative JOA score). A recovery rate >50 % was defined as an effective clinical result in JOA score [16, 17].

Table 1 Quick Disabilities of the Arm, Shoulder, and Hand (QuickDASH) questionnaire

Question no.	Item
qDASH-1	Open a tight or new jar
qDASH-2	Do heavy household chores (e.g., wash walls, wash floors)
qDASH-3	Carry a shopping bag or briefcase
qDASH-4	Wash your back
qDASH-5	Use a knife to cut food
qDASH-6	Recreational activities that require little effort (e.g., card playing, knitting, etc.)
qDASH-7	During the past week, to what extent has your arm, shoulder, or hand problem interfered with your normal social activities with family, friends, neighbors, or groups?
qDASH-8	During the past week, were you limited in your work or other daily activities as a result of your arm, shoulder, or hand problem?
qDASH-9	Arm, shoulder, or hand pain
qDASH-10	Tingling (pins and needles) in your arm, shoulder, or hand
qDASH-11	During the past week, how much difficulty have you had sleeping because of the pain in your arm, shoulder, or hand?

Table 2 Scoring system for cervical myelopathy proposed by the Japanese Orthopaedic Association (JOA score)

Motor dysfunction of the upper extremity
Score
0. Cannot eat with spoon
1. Can eat with a spoon, but not with chopsticks
2. Can eat with chopsticks, to a limited degree
3. Can eat with chopsticks, but awkward
4. No disability
Motor dysfunction of the lower extremity
Score
0. Cannot walk
1. Needs cane or aid on flat ground
2. Needs cane or aid only on stairs
3. Can walk without cane or aid, but slowly
4. No disability
Sensory deficit
A. Upper extremities
Score
0. Severe sensory loss or pain
1. Mild sensory loss
2. None
B. Lower extremities same as A
C. Trunk same as A
Sphincter dysfunction
Score
0. Unable to void
1. Marked difficulty in micturition (retention, strangury)
2. Difficulty in micturition (pollakiuria, hesitation)
3. None

Statistical analysis

SPSS version 17 software (SPSS Inc., Chicago, IL, USA) was used to perform statistical analyses. Internal consistency was evaluated by Cronbach α. The criterion-related validity was evaluated by calculating correlation coefficients (Spearman's ρ) between QuickDASH and other outcome measures; Student's t test, Mann–Whitney U test, Pearson's correlation coefficient, and chi-square test were used to evaluate the association between groups. Differences were considered significant at $P < 0.05$.

We also plotted the receiver operating characteristic (ROC) curves to investigate the QuickDASH cutoff value for patient satisfaction with cervical laminoplasty.

Results

The mean JOA score w as 10.1 (range 3–15) points before surgery and 13.3 (range 3–17) points after surgery. Mean JOA recovery rate was 46.2 % (range 0–100 %). Preoperative and postoperative average JOA scores were 2.4 ± 0.8 and 3.3 ± 0.8, respectively, for upper-extremity motor function and 0.8 ± 0.4 and 1.1 ± 0.5, respectively, for upper-extremity sensory function. Total JOA score and subscore for the upper extremities improved significantly after surgery ($P < 0.05$). The average postoperative QuickDASH score was 30.0 (range 0–100) points. Cronbach α of QuickDASH was 0.94, which is generally regarded as an excellent score. Table 3 shows correlations between QuickDASH and outcomes; QuickDASH showed significant correlation with outcomes from all the other assessment scales, particularly with NDI and SF-36 ($r > 0.75$).

We then determined the QuickDASH cutoff value for patient satisfaction as an endpoint. According to ROC curve analysis, a cutoff value of 34.0 gave the maximum power of QuickDASH for assessing patient satisfaction based on clinical results with cervical laminoplasty [area under the curve (AUC) 0.730] (Fig. 1).

We classified the patients into two groups according to treatment satisfaction. Patients who chose "neither" were classified into the not satisfied group. The satisfied group comprised 57 patients, and the not satisfied group comprised 37. QuickDASH score, JOA score for upper-extremity sensory function, and recovery rate were significantly better in the satisfied group than in the not satisfied group. However, there was no significant difference in JOA score for upper-extremity motor function between groups (Table 4).

Discussion

This study was conducted to evaluate the validity of QuickDASH as a measure of functional status of the upper extremity for patients after cervical laminoplasty. Results show that QuickDASH had significant correlations not only with disease-specific JOA scores but also with other generic patient-reported outcome measures. In addition, QuickDASH had an excellent correlative coefficient and significantly reflected patient satisfaction with treatment, whereas the JOA score for the upper-extremity motor function did not.

Upper-extremity function is affected by many factors, such as dexterity, weakness, numbness, and paresthesia. It is difficult to strictly divide the upper extremities into distinct parts, such as arm, shoulder, hand, neck, and scapular. Our results show that the QuickDASH was suitable for comprehensively evaluating symptoms and functional status of the upper extremities. In contrast, the JOA score is an ordinal variable, not a continuous variable, and the subscore is expressed as only 5 (motor) or 3 (sensory)

Table 3 Correlation between Quick Disabilities of the Arm, Shoulder, and Hand (QuickDASH) self-report questionnaire and other test outcomes

	Correlation coefficient	*P* value
JOA score		
Motor (U/E)	−0.495	<0.01
Sensory (U/E)	−0.324	<0.01
Recovery rate	−0.509	<0.01
SF-36(PCS)	−0.753	<0.01
NRS (pain in U/E)	0.693	<0.01
NDI	0.834	<0.01

JOA Japan Orthopedic Association, *U/E* upper extremities, *PCS* physical component score, *NRS* Numeric Rating Scale, *NDI* Neck Disability Index

Table 4 Comparison between groups

	Satisfied	Not satisfied	*P* value
QuickDASH	23.2	40.5	<0.01
JOA score			
Motor (U/E)	3.4	3.2	N.S.
Sensory (U/E)	1.2	1	0.03
SF-36 (PCS)	36.3	27.6	0.02
NRS (pain in U/E)	2.2	4.6	<0.01
NDI	21.8	37.3	<0.01

QuickDASH Quick Disabilities of the Arm, Shoulder, and Hand, *U/E* upper extremity, *SF-36* Short-Form Health Questionnaire of 36 questions, *PCS* physical component score, *NRS* Numeric Rating Scale, *NDI* Neck Disability Index

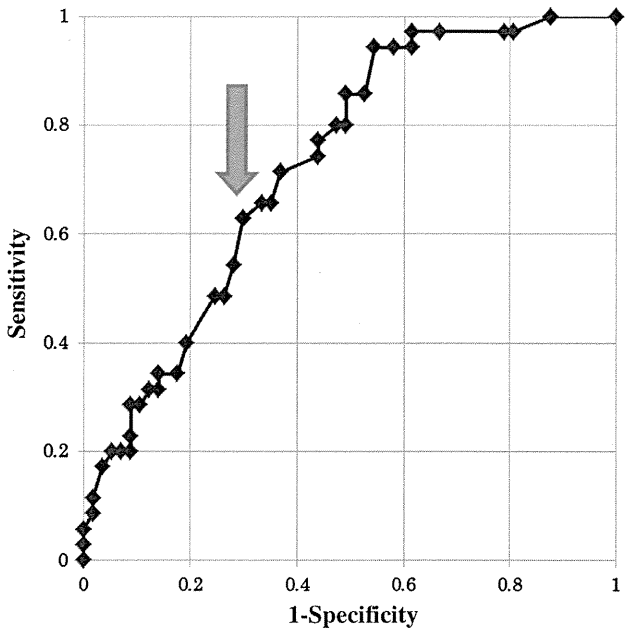

Fig. 1 Receiver Operating Characteristics (ROC) curve for determining the cutoff value for patient satisfaction following cervical laminoplasty. The *arrow* indicates the plotted point that determines the cutoff value

discrete variables [18]. This may be why the JOA score for the upper-extremity motor function did not affect postoperative satisfaction.

Several performance tests have been developed for objectively assessing the severity of hand myelopathy. For example, Kimura et al. [19] proposed the tally counter test, and Hosono et al. [20] proposed the 15-s grip–release test in addition to the conventional 10-s test. These tests are simple, reliable, and capable of detecting small functional changes. However, they do not evaluate sensory function or provide patient-reported outcomes. On the other hand, the QuickDASH is a patient-reported outcome, and we must evaluate the correlation between the QuickDASH and the other objective evaluations, such as these performance tests.

We determined the QuickDASH cutoff value to be 34.0. Although we had no preoperative QuickDASH data, the value obtained is considered to be reasonable because the mean QuickDASH scores were reported to be approximately 30 in the studies that evaluated patients with upper-extremity disorders [8]. We used patient satisfaction as an endpoint in order to determine the QuickDASH cutoff value.

However, it must also be affected by the function of the lower extremities or the degree of recovery. Preoperative QuickDASH scores are also required.

There were some limitations in this study. First, it was a retrospective design, and the relatively low follow-up rate indicates the possibility of patient selection bias. Second, there were no preoperative outcomes except for JOA score. To precisely investigate the reliability and responsiveness of the QuickDASH questionnaire to assess cervical surgery outcomes, we need to evaluate both pre- and postoperative outcomes. Finally, there are variations in the follow-up period (range 12–274 months). Late neurologic deterioration after laminoplasty is well known [4]. In order to avoid the effects of aging, outcome evaluation should take place in all patients at the same time period after operation. Also, for the same reason, comparison between QuickDASH assessment of cervical myelopathy patients and that of an age-matched control is required. However, there are no significant correlations ($r = 0.2$) between QuickDASH and the follow-up periods in this study. Imaeda et al. reported the low correlation between QuickDASH and age in their study group, so the aging effect on function may be negligible in our study. Some changes may also occur in the procedure or postoperative therapy during the long follow-up period. Our procedure was basically C3-7 laminoplasty with the hydroxyapatite (HA) spacer, and we think that

such changes across time did not affect postoperative function of the upper extremities.

Nevertheless, we regard QuickDASH as a reliable tool for obtaining patient-reported outcomes in evaluations of cervical interventions, not only because the QuickDASH scores had significant correlations with other disease-specific and general outcomes commonly used for assessing cervical diseases but also because Cronbach α for QuickDASH was excellent and reliable.

One possible problem in using QuickDASH is the influence of lower-limb function. Dowrick et al. [21] reported that the DASH score also measured disability in patients with injuries to the lower limb, and care must be taken when attributing disability measured by the DASH score to injuries of the upper limb if problems are also present in the lower limb. In fact, the QuickDASH questionnaire includes some items that must be influenced by lower-extremity function. For example, question no. 3, "Carry the shopping bag or briefcase," includes two actions: holding the bag and walking at the same time. Taking these factors into consideration, the significant correlation between QuickDASH and the other assessment outcomes may have been affected by lower-extremity function.

Finally, this study provides evidence to support the use of QuickDASH to measure upper-extremity symptoms and disability in patients with cervical surgery. The use of this questionnaire to obtain patient-reported outcomes allows subtle but significant changes in the upper extremity to be detected, which can truly reflect patient satisfaction with treatment.

Acknowledgments The authors thank patients and and their families for allowing us to present the clinical data reported here.

Conflict of interest No benefits in any form have been received or will be received from a commercial party related directly or indirectly to the subject of this article.

References

1. Bernhardt M, Hynes RA, Blume HW, White AA. Cervical spondylotic myelopathy. J Bone Joint Surg Am. 1993;75:119–28.
2. Yonenobu K, Fuji T, Ono K, Okada K, Yamamoto T, Harada N. Choice of surgical treatment for multisegmental cervical spondylotic myelopathy. Spine (Phila Pa 1976). 1985;10:710–6.
3. Chiba K, Ogawa Y, Ishii K, Takaishi H, Nakamura M, Maruiwa H, Matsumoto M, Toyama Y. Long-term results of expansive open-door laminoplasty for cervical myelopathy–average 14-year follow-up study. Spine (Phila Pa 1976). 2006;31:2998–3005.
4. Seichi A, Takeshita K, Ohishi I, Kawaguchi H, Akune T, Anamizu Y, Kitagawa T, Nakamura K. Long-term results of double-door laminoplasty for cervical stenotic myelopathy. Spine (Phila Pa 1976). 2001;26:479–87.
5. Chiba K, Toyama Y, Matsumoto M, Maruiwa H, Watanabe M, Hirabayashi K. Segmental motor paralysis after expansive open-door laminoplasty. Spine (Phila Pa 1976). 2002;27:2108–15.
6. Sakaura H, Hosono N, Mukai Y, Ishii T, Yoshikawa H. C5 palsy after decompression surgery for cervical myelopathy: review of the literature. Spine (Phila Pa 1976). 2003;28:2447–51.
7. Beaton DE, Wright JG, Katz JN, Group UEC. Development of the QuickDASH: comparison of three item-reduction approaches. J Bone Joint Surg Am. 2005;87:1038–46.
8. Imaeda T, Toh S, Wada T, Uchiyama S, Okinaga S, Kusunose K, Sawaizumi T. Impairment Evaluation Committee JpSfSotH. Validation of the Japanese Society for Surgery of the Hand Version of the Quick Disability of the Arm, Shoulder, and Hand (QuickDASH-JSSH) Questionnaire. J Orthop Sci. 2006;11:248–53.
9. Gummesson C, Atroshi I, Ekdahl C. The disabilities of the arm, shoulder and hand (DASH) outcome questionnaire: longitudinal construct validity and measuring self-rated health change after surgery. BMC Musculoskelet Disord. 2003;4:11.
10. Huisstede BM, Feleus A, Bierma-Zeinstra SM, Verhaar JA, Koes BW. Is the disability of arm, shoulder, and hand questionnaire (DASH) also valid and responsive in patients with neck complaints. Spine (Phila Pa 1976). 2009;34:E130–8.
11. Mehta S, Macdermid JC, Carlesso LC, McPhee C. Concurrent validation of the DASH and the QuickDASH in comparison to neck-specific scales in patients with neck pain. Spine (Phila Pa 1976). 2010;35:2150–6.
12. Fukuhara S, Bito S, Green J, Hsiao A, Kurokawa K. Translation, adaptation, and validation of the SF-36 health survey for use in Japan. J Clin Epidemiol. 1998;51:1037–44.
13. Fukuhara S, Ware JE, Kosinski M, Wada S, Gandek B. Psychometric and clinical tests of validity of the Japanese SF-36 health survey. J Clin Epidemiol. 1998;51:1045–53.
14. Vernon H, Mior S. The neck disability index: a study of reliability and validity. J Manip Physiol Ther. 1991;14:409–15.
15. Hirabayashi K, Miyakawa J, Satomi K, Maruyama T, Wakano K. Operative results and postoperative progression of ossification among patients with ossification of cervical posterior longitudinal ligament. Spine (Phila Pa 1976). 1981;1981(6):354–64.
16. Satomi K, Nishu Y, Kohno T, Hirabayashi K. Long-term follow-up studies of open-door expansive laminoplasty for cervical stenotic myelopathy. Spine (Phila Pa 1976). 1994;19:507–10.
17. Kohno K, Kumon Y, Oka Y, Matsui S, Ohue S, Sakaki S. Evaluation of prognostic factors following expansive laminoplasty for cervical spinal stenotic myelopathy. Surg Neurol. 1997;48:237–45.
18. Suzuki A, Misawa H, Simogata M, Tsutsumimoto T, Takaoka K, Nakamura H. Recovery process following cervical laminoplasty in patients with cervical compression myelopathy: prospective cohort study. Spine (Phila Pa 1976). 2009;34:2874–9.
19. Kimura A, Seichi A, Endo T, Norimatsu Y, Inoue H, Higashi T, Hoshino Y. Tally counter test as a simple and objective assessment of cervical myelopathy. Eur Spine J. 2013;22:183–8.
20. Hosono N, Takenaka S, Mukai Y, Makino T, Sakaura H, Miwa T, Kaito T. Postoperative 24-hour result of 15-second grip-and-release test correlates with surgical outcome of cervical compression myelopathy. Spine (Phila Pa 1976). 2012;37:1283–7.
21. Dowrick AS, Gabbe BJ, Williamson OD, Cameron PA. Does the disabilities of the arm, shoulder and hand (DASH) scoring system only measure disability due to injuries to the upper limb? J Bone Joint Surg Br. 2006;88:524–7.

Published December 23, 2013

JEM

Article

Bone resorption is regulated by cell-autonomous negative feedback loop of Stat5–Dusp axis in the osteoclast

Jun Hirose,[1] Hironari Masuda,[1] Naoto Tokuyama,[1] Yasunori Omata,[1] Takumi Matsumoto,[1] Tetsuro Yasui,[1] Yuho Kadono,[1] Lothar Hennighausen,[2] and Sakae Tanaka[1]

[1]Department of Orthopaedic Surgery, Faculty of Medicine, The University of Tokyo, Bunkyo-ku, Tokyo 113-0033, Japan
[2]Laboratory of Genetics and Physiology, National Institute of Diabetes and Digestive and Kidney Diseases, National Institutes of Health, Bethesda, MD 20892

Signal transducer and activator of transcription 5 (Stat5) is essential for cytokine-regulated processes such as proliferation, differentiation, and survival in hematopoietic cells. To investigate the role of Stat5 in osteoclasts, we generated mice with an osteoclast-specific conditional deletion of *Stat5* (*Stat5* conditional knockout [cKO] mice) and analyzed their bone phenotype. *Stat5* cKO mice exhibited osteoporosis caused by an increased bone-resorbing activity of osteoclasts. The activity of mitogen-activated protein kinases (MAPKs), in particular extracellular signal–related kinase, was increased in *Stat5* cKO osteoclasts, whereas the expression of the MAPK phosphatases dual specificity phosphatase 1 (Dusp1) and Dusp2 was significantly decreased. Interleukin-3 (IL-3) stimulated the phosphorylation and nuclear translocation of Stat5 in osteoclasts, and Stat5 expression was up-regulated in response to receptor activator of nuclear factor κB ligand (RANKL). The results suggest that Stat5 negatively regulates the bone-resorbing function of osteoclasts by promoting Dusp1 and Dusp2 expression, and IL-3 promotes Stat5 activation in osteoclasts.

CORRESPONDENCE
Sakae Tanaka:
TANAKAS-ORT@h.u-tokyo.ac.jp

Abbreviations used: cKO, conditional KO; CT, computed tomography; DXA, dual-energy x-ray absorptiometry; MAPK, mitogen-activated protein kinase; MKP, MAPK phosphatase; RANKL, receptor activator of NF-κB ligand; TRAP, tartrate-resistant acid phosphatase.

Bone is a dynamic tissue that undergoes constant remodeling, balancing bone resorption by osteoclasts with bone formation by osteoblasts (Baron, 1989; Karsenty and Wagner, 2002). An altered balance between bone formation and bone resorption causes diseases such as osteoporosis and osteopetrosis (Seeman, 2003; Villa et al., 2009). It is well known that osteoclasts are responsible for the pathological bone resorption in various diseases, including rheumatoid arthritis, the loosening of artificial joints, and osteolysis in metastatic cancers (Takayanagi et al., 2000; Roodman, 2004; Sommer et al., 2005; Tanaka, 2007). Osteoclasts are multinucleated bone-resorbing cells derived from hematopoietic precursors of the monocyte-macrophage lineage, and their differentiation is induced by M-CSF and receptor activator of NF-κB ligand (RANKL; Lacey et al., 1998; Yasuda et al., 1998; Suda et al., 1999). RANKL is not only important for the differentiation of osteoclasts, but it also regulates their bone-resorbing activity and survival. Although bone resorption is tightly regulated in the skeletal milieu, the molecular mechanisms underlying it are not fully understood.

The Stat family of transcription factors conveys cytokine signals from the respective membrane receptors to the nucleus, where they activate diverse genetic programs (Akira, 1999). Stat5 was originally identified as mammary gland factor (MGF), implying a specificity to the physiology of mammary tissue (Wakao et al., 1994). Two members of the Stat family, Stat5a and Stat5b (collectively called Stat5), have gained prominence in that they are activated by a wide variety of cytokines (Hennighausen and Robinson, 2008). Stat5a and Stat5b play redundant and nonredundant roles that are essential in a variety of cytokine responses (Teglund et al., 1998). Recently, it was demonstrated that

The Rockefeller University Press $30.00
J. Exp. Med. 2014 Vol. 211 No. 1 153-163
www.jem.org/cgi/doi/10.1084/jem.20130538

Published December 23, 2013

Stat5 has important functions in immune cell development. Mice completely lacking Stat5 failed to develop T or B lymphocytes as well as NK cells (Hoelbl et al., 2006; Yao et al., 2006), and *Stat5*-null embryos are perinatally lethal, possibly as the result of severe anemia (Cui et al., 2004). Stat5 also plays an essential role in certain pathological conditions. Activated STAT5 was detected in BCR-ABL–induced chronic myeloid leukemia (Ilaria and Van Etten, 1996), and a recent study reported that activated Stat5 was detected in the blast cells of acute myeloblastic leukemia and acute lymphoblastic leukemia patients (Van Etten, 2007). These results suggest that Stat5 plays an essential role in a variety of cells, particularly of the hematopoietic lineage. However, the role of Stat5 in osteoclasts has yet to be elucidated.

In this study, we investigated the roles of Stat5 in osteoclasts in vivo and in vitro. It was demonstrated that Stat5 negatively regulates the bone-resorbing activity of osteoclasts and that osteoclast-specific *Stat5* KO mice exhibited reduced bone mass. We identified dual specificity mitogen-activated protein kinase (MAPK) phosphatase 1 (Dusp1) and Dusp2 as targets of Stat5. Only IL-3 among the known stimulators activated Stat5 and induced the expression of both Dusp1 and Dusp2. IL-3 expression is up-regulated in osteoclasts in response to RANKL, thus providing a cell-autonomous negative feedback loop in bone resorption.

RESULTS

Stat5 conditional KO (cKO) mice exhibit decreased bone mass

To investigate the role of Stat5 in osteoclasts, we generated osteoclast-specific *Stat5a&b* cKO (*Stat5* cKO) mice by mating $Stat5^{fl/fl}$ mice (Cui et al., 2004) with cathepsin K–Cre transgenic mice, in which the Cre recombinase gene is inserted into the *cathepsin K* locus and specifically expressed in osteoclasts (Nakamura et al., 2007). *Stat5* cKO mice were born alive at predicted Mendelian frequencies. Stat5 expression was barely observed in osteoclasts from the *Stat5* cKO mice (Fig. 1 A), whereas its expression in other tissues was comparable with that in the $Stat5^{fl/fl}$ littermates (not depicted). *Stat5* cKO mice grew normally with no apparent morphological abnormalities (Fig. 1 B) and they exhibited a normal height and weight (Fig. 1 C). In addition, the serum levels of growth hormone or insulin like growth factor I (IGF-I) in *Stat5* cKO mice were within normal range and exhibited no significant difference from normal littermates (Fig. 1 D). 1-yr-old male *Stat5* cKO mice exhibited a decreased bone mass in the proximal tibia and lumbar spine, as shown by radiography (Fig. 1 E) and dual-energy x-ray absorptiometry (DXA; Fig. 1 F). Microcomputed tomography (micro-CT) analysis of the distal femur revealed apparent osteopenia in the *Stat5* cKO male mice at 1 yr of age. Bone volume/tissue volume (BV/TV) and trabecular number (Tb.N) were significantly reduced, and trabecular separation (Tb.Sp) significantly increased in 1-yr-old *Stat5* cKO mice compared with $Stat5^{fl/fl}$ mice (Fig. 1 G). These data suggest that Stat5 signaling plays an important role in regulating bone homeostasis.

Bone resorption is increased in *Stat5* cKO mice

Histological and histomorphometric analyses revealed that a decrease in trabecular bone volume was already taking place in 8-wk-old *Stat5* cKO male mice compared with $Stat5^{fl/fl}$ mice (Fig. 2, A and B). 8-wk-old *Stat5* cKO female mice exhibited a significantly decreased Tb.N and an increased Tb.Sp, whereas BV/TV was not significantly different between cKO mice and control mice (not depicted). The *Stat5* cKO male mice exhibited a significant increase in the eroded surface/bone surface (ES/BS) and osteoclast surface/bone surface (Oc.S/BS), but not in osteoclast number (Oc.N/B.Pm), as shown by tartrate-resistant acid phosphatase (TRAP) staining of bone sections and histomorphometric analysis (Fig. 2 C). In contrast, the bone formation parameters, mineral apposition rate (MAR) and bone formation rate (BFR/BS), did not exhibit any significant difference between *Stat5* cKO mice and $Stat5^{fl/fl}$ mice (Fig. 2 D). The serum levels of C-terminal cross-linking telopeptide of type 1 collagen (CTx-I), a bone resorption marker, were significantly increased in *Stat5* cKO mice compared with $Stat5^{fl/fl}$ mice, whereas the serum levels of osteocalcin, a bone formation marker, were equivalent to those in $Stat5^{fl/fl}$ mice (Fig. 2 E). These findings suggest that bone loss in *Stat5* cKO mice is caused by an increased bone-resorbing activity of osteoclasts, rather than by decreased bone formation.

Stat5 negatively regulates osteoclast function

To clarify the mechanism of increased bone resorption by Stat5 deletion, we performed in vitro experiments using BM cells isolated from *Stat5* cKO and $Stat5^{fl/fl}$ mice. We first evaluated whether the M-CSF–dependent proliferation of BM cells was different between *Stat5* cKO and $Stat5^{fl/fl}$ mice by MTT assay. Proliferation was comparable between cells from $Stat5^{fl/fl}$ mice and those from *Stat5* cKO mice (not depicted). The RANKL-induced osteoclastic differentiation of BM cells from Stat5 cKO mice did not differ from cells from $Stat5^{fl/fl}$ mice, as demonstrated by TRAP staining (Fig. 3 A), the $TRAP^+$ multinucleated cell number (Fig. 3 B), and the expression of osteoclast differentiation markers (*Nfatc1*, *Ctsk*, and *Acp5*; not depicted). We next evaluated the bone-resorbing activity of fully differentiated osteoclasts by pit formation assay on dentine slices. Osteoclasts differentiated from the BM cells of the *Stat5* cKO mice (*Stat5* cKO osteoclasts) exhibited an increased bone-resorbing activity compared with osteoclasts from the $Stat5^{fl/fl}$ mice ($Stat5^{fl/fl}$ osteoclasts; Fig. 3 C). The increased bone-resorbing activity of *Stat5* cKO osteoclasts was hindered by the adenoviral reintroduction of Stat5a/b (Fig. 3 D). Inversely, Stat5 overexpression significantly reduced the bone-resorbing activity of osteoclasts (Fig. 3 E). The size or actin organization did not differ apparently between Stat5 cKO and $Stat5^{fl/fl}$ osteoclasts on dentin slices, though the size is quite different between individual osteoclast (Fig. 3 F). We then generated osteoclasts from *Stat5* cKO mice BM cells by stimulating these cells with M-CSF and RANKL and examined the effect of Stat5 deficiency on osteoclast survival. As shown in Fig. 3 G, the loss of Stat5 did

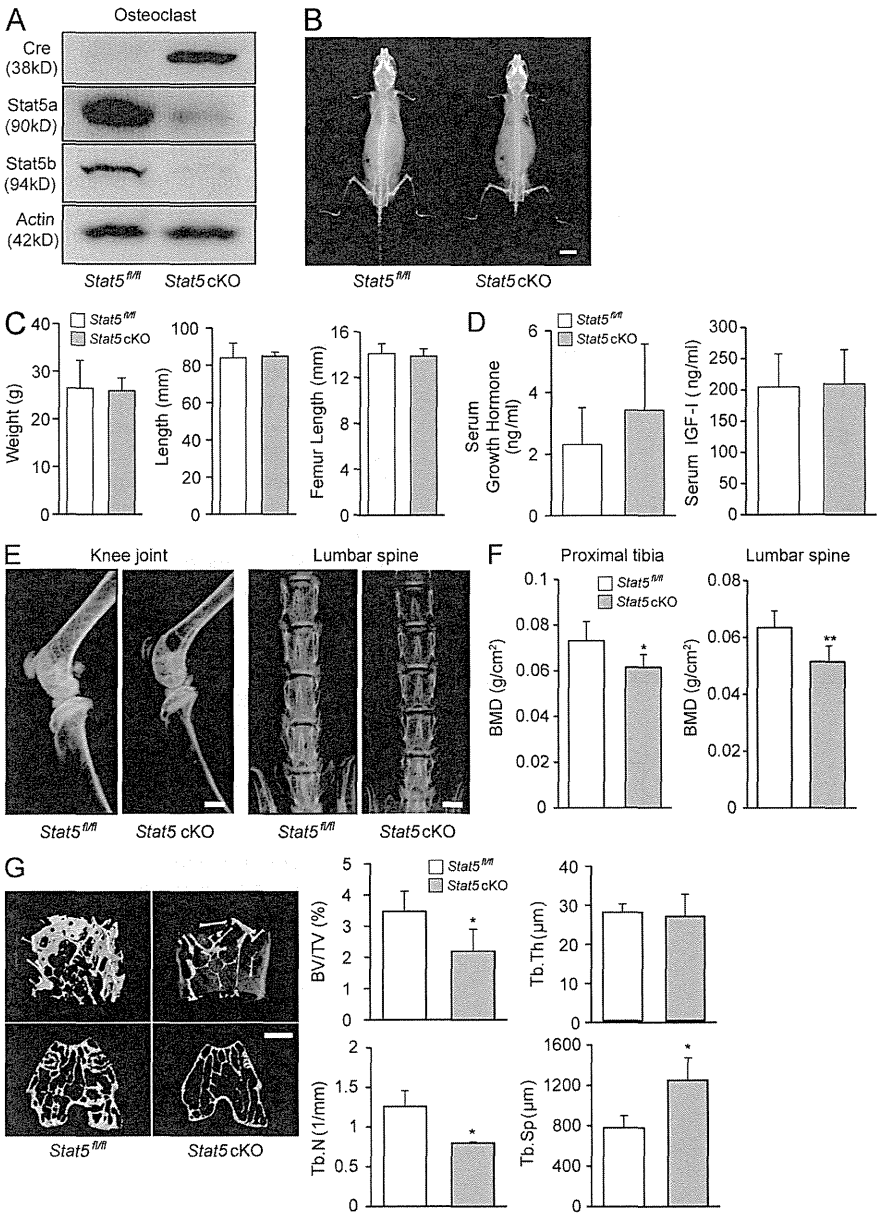

Figure 1. *Stat5* cKO mice exhibit decreased bone mass. (A) Expression of Cre recombinase and Stat5 in osteoclasts from *Stat5*$^{fl/fl}$ mice and *Stat5* cKO mice was analyzed by Western blotting. β-Actin was used as an internal control. (B) Radiographs of a *Stat5*$^{fl/fl}$ male mouse (left) and a *Stat5* cKO male mouse (right) at 3 mo of age. (C) Body weight and length and femur length were measured for 12-wk-old *Stat5*$^{fl/fl}$ and *Stat5* cKO male mice. Data are the mean ± SD ($n = 4$). (D) Serum levels of growth hormone (left) and IGF-I (right) in *Stat5*$^{fl/fl}$ mice and *Stat5* cKO mice were measured by ELISA. Data are represented as the mean ± SD ($n = 6$). (E) Representative x-ray images of the knee joint and lumbar spine of a *Stat5*$^{fl/fl}$ male mouse (left) and a *Stat5* cKO male mouse (right) at 1 yr of age. (F) Bone mineral density (BMD) of the distal femur and lumbar spine of 1-yr-old *Stat5*$^{fl/fl}$ male mice and *Stat5* cKO male mice was determined by DXA. Data are the mean ± SD (*, $P < 0.05$; **, $P < 0.01$; $n = 6$). (G) Representative micro-CT images of the distal femur in a *Stat5*$^{fl/fl}$ mouse (left) and *Stat5* cKO mouse (right) at 1 yr of age. Graphs show quantitative data from the CT analyses. BV/TV, bone volume per total volume; Tb.N, trabecular number; Tb.Th, trabecular thickness; Tb.Sp, trabecular separation. Data are represented as the mean ± SD (*, $P < 0.05$; $n = 3$). Bars: (B) 1 cm; (E and G) 1 mm.

not affect the osteoclast survival rate or apoptosis of osteoclasts evaluated by TUNEL staining. The expression of cleaved caspase-3, a primary caspase in the execution of apoptosis, was also not significantly different (not depicted). These results suggest that Stat5 is essential for the bone-resorbing activity but not the differentiation or survival of osteoclasts.

Stat5 suppresses MAPK activity by regulating the expression of *Dusp1* and *Dusp2* in osteoclasts

To examine the mechanisms underlying the increase in the bone-resorbing activity of *Stat5* cKO osteoclasts, we first analyzed the intracellular signaling pathways. As assessed by Western blotting, the phosphorylation of MAPs, in particular extracellular signal–related kinase 1/2 (ERK1/2), was increased in *Stat5* cKO osteoclasts as compared with *Stat5*$^{fl/fl}$ osteoclasts, whereas the phosphorylation of IκBα, Akt, and c-Src was unchanged by Stat5 deletion (Fig. 4 A). Conversely, retroviral vector–mediated overexpression of Stat5a/b resulted in a diminished MAPK activity (Fig. 4 B).

To uncover the molecular mechanisms of MAPK regulation by Stat5, we undertook comparative microarray screens of *Stat5*$^{fl/fl}$ and *Stat5* cKO osteoclasts. Among the genes whose expression was reduced in *Stat5* cKO osteoclasts to less than half of that in *Stat5*$^{fl/fl}$ osteoclasts, we focused on *Dusp2*. The Dusps are a heterogeneous group of protein phosphatases that dephosphorylate both phosphotyrosine and phosphoserine/phosphothreonine residues within one substrate. Many of the Dusps serve as MAPK phosphatases (MKPs), which

Published December 23, 2013

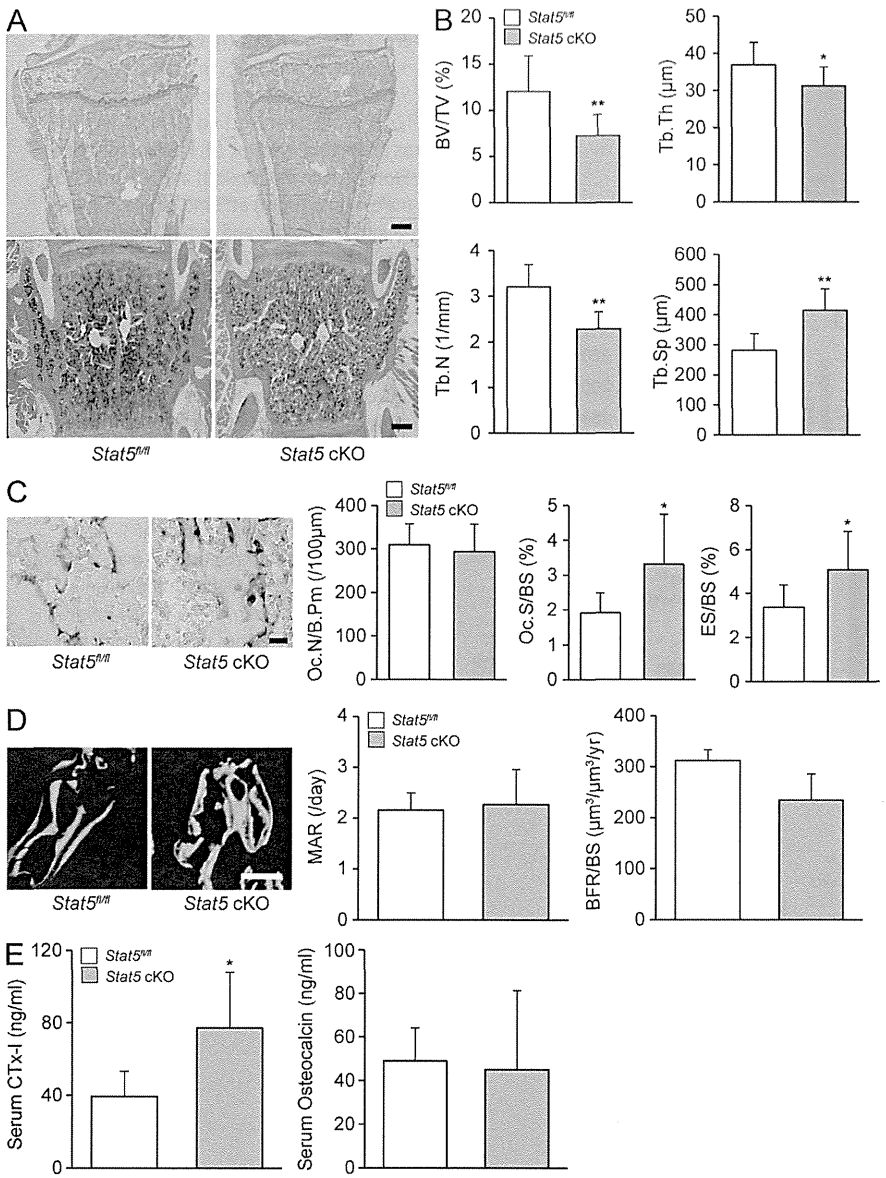

Figure 2. Bone resorption was promoted in *Stat5* cKO mice. (A) Undecalcified sections of the proximal tibia (top) or decalcified section of the lumbar spine (bottom) from 8-wk-old *Stat5*$^{fl/fl}$ male mice (left) or *Stat5* cKO male mice (right) were stained with toluidine blue (top) or H&E (bottom). Representative images from three mice/group are shown. (B) Histomorphometric analyses were performed on 8-wk-old *Stat5*$^{fl/fl}$ male mice and *Stat5* cKO male mice. BV/TV, bone volume per total volume; Tb.Th, trabecular thickness; Tb.N, trabecular number; Tb.Sp, trabecular separation. Data are represented as the mean ± SD (*, $P < 0.05$; **, $P < 0.01$; $n = 6$). (C) TRAP expression in tibia from *Stat5*$^{fl/fl}$ (left) or *Stat5* cKO mice (right) was assessed by TRAP staining and the following parameters were measured: Oc.N/B.Pm, osteoclast number per bone perimeter; Oc.S/BS, osteoclast surface per bone surface; ES/BS, eroded surface per bone surface. Data are represented as the mean ± SD (*, $P < 0.05$; $n = 6$). (D) Dynamic histomorphometric analysis of *Stat5*$^{fl/fl}$ and *Stat5* cKO mice was performed after mice were injected subcutaneously with 16 mg/kg body weight of calcein at −3 and −1 d before sacrifice. Graphs show MAR, mineral apposition rate; BFR/BS, bone formation rate per bone surface. Data are represented as the mean ± SD ($n = 6$). (E) Serum concentration of CTx-I and osteocalcin in *Stat5*$^{fl/fl}$ mice and *Stat5* cKO mice was assessed by ELISA. Data are represented as the mean ± SD (*, $P < 0.05$; $n = 4$/group). Bars: (A and D) 100 μm; (C) 25 μm.

dephosphorylate MAPKs with substrate specificity. Real-time PCR analysis in *Stat5*$^{fl/fl}$ and *Stat5* cKO osteoclasts revealed that among the Dusps with MKP activity, the expression of *Dusp1* and *Dusp2* was significantly reduced in *Stat5* cKO osteoclasts (Fig. 4 C). Overexpression of either Stat5a or Stat5b increased the expression of *Dusp1* and *Dusp2*, with Stat5a exhibiting stronger activity (Fig. 4 D). The increased bone-resorbing activity of *Stat5* cKO osteoclasts was disrupted by the adenoviral reintroduction of Dusp1 and Dusp2 (Fig. 4 E). To examine the MKP activity of Dusp1 and Dusp2 in osteoclasts, we overexpressed Dusp1 and Dusp2 using retrovirus vectors. As shown in Fig. 4 F, Dusp1-overexpressing osteoclasts exhibited decreased activity of ERK, JNK, and p38, whereas Dusp2-overexpressing cells exhibited decreased activity of ERK and mildly increased activity of JNK and p38 (Fig. 4 F). These results suggest that the increased activity of MAPKs in *Stat5* cKO osteoclasts was caused by the decreased expression of Dusp1 and Dusp2, which in turn resulted in their increased bone-resorbing activity.

IL-3 is a possible stimulator of Stat5 in osteoclasts

To identify factors that activate Stat5 in osteoclasts, we examined the effects of various cytokines or growth factors on Stat5 phosphorylation. Among the known stimulators of Stat5 (IL-2, IL-3, IL-5, IL-7, GM-CSF, GH, and PRL), IL-3 and GM-CSF induced Stat5 phosphorylation in osteoclasts, although the time course of Stat5 phosphorylation by GM-CSF was more rapid and temporary than that by IL-3 (Fig. 5 A). To determine the effect of these cytokines on bone resorptive activity of osteoclasts, pit formation assay was performed under the presence of IL-3 and GM-CSF. As shown in Fig. 5 B, bone resorption was suppressed by IL-3 but not by GM-CSF

Published December 23, 2013

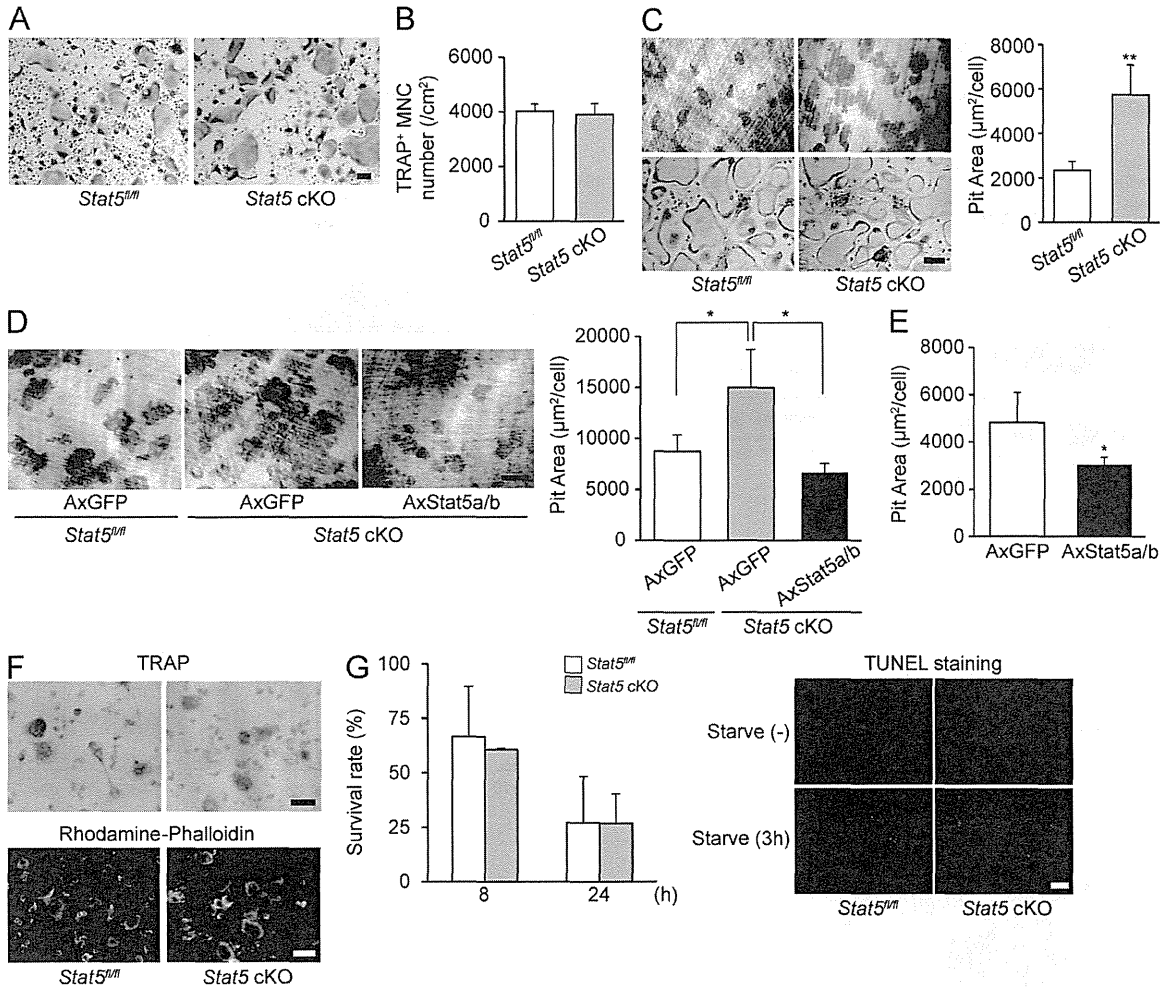

Figure 3. Stat5 suppresses the bone-resorbing activity of osteoclasts. (A) BMDMs from *Stat5*$^{fl/fl}$ mice and *Stat5* cKO mice were cultured in the presence of M-CSF and RANKL for 4 d, and cultures were stained for TRAP$^+$ cells. (B) BMDMs from *Stat5*$^{fl/fl}$ mice and *Stat5* cKO mice were cultured in the presence of M-CSF and RANKL for 4 d, and the TRAP$^+$ multinucleated cells (MNCs) containing more than three nuclei were counted as osteoclasts. Data are represented as the mean ± SD ($n = 3$). (C) Osteoclasts from *Stat5*$^{fl/fl}$ and *Stat5* cKO mice were cultured on dentine slices for 24 h, and the resorption areas were visualized by staining with toluidine blue staining and measured using an image analysis system. Representative resorption pits and TRAP staining of parallel cultures are shown (left). Graph shows pit resorption area per osteoclast (right). Data are represented as the mean ± SD (**, $P < 0.01$; $n = 3$). (D) Osteoclasts from *Stat5*$^{fl/fl}$ or *Stat5* cKO mice infected with AxGFP or AxStat5a/b were cultured on dentine slices for 24 h, and the resorption areas were visualized by staining with toluidine blue staining. Pit resorption area per osteoclast and representative resorption pits are shown. Data are represented as the mean ± SD (*, $P < 0.05$; $n = 3$). (E) Osteoclasts from WT mice infected with AxGFP or AxStat5a/b were cultured on dentine slices for 24 h, and the resorption areas were visualized by staining with toluidine blue staining. Graph shows pit resorption area per osteoclast. Data are represented as the mean ± SD (*, $P < 0.05$; $n = 3$). (F) TRAP staining and rhodamine-conjugated phalloidin staining of osteoclasts from *Stat5*$^{fl/fl}$ mice and *Stat5* cKO mice on dentin slices. (G) *Stat5*$^{fl/fl}$ and *Stat5* cKO osteoclasts were cultured for 8 or 24 h after cytokine withdrawal (left). Apoptosis of osteoclasts from *Stat5*$^{fl/fl}$ and *Stat5* cKO mice after 0- and 3-h serum starvation was assessed by TUNEL staining. Data are represented as the mean ± SD ($n = 3$). (A, C, D, F, and G) Bars, 100 μm. Results in all panels are representative of two independent experiments.

stimulation (Fig. 5 B). Therefore, we hypothesized that IL-3–induced activation of Stat5 negatively regulates osteoclast function. Supporting this hypothesis, nuclear translocation of Stat5 was observed in response to IL-3 stimulation (Fig. 5 C). Real-time RT-PCR demonstrated that IL-3 induced a rapid increase in *Dusp1* and *Dusp2* mRNA in WT osteoclasts, whereas this induction was much reduced in *Stat5* cKO osteoclasts (Fig. 5 D). We also found that IL-3 inhibits bone-resorbing activity of *Stat5*$^{fl/fl}$ osteoclasts, but bone-resorbing activity of *Stat5* cKO osteoclasts was not affected by IL-3, as shown in Fig. 5 E. Interestingly, the expression of *IL-3* was rapidly induced in osteoclasts in response to RANKL stimulation (Fig. 5 F). These data suggest that the IL-3 produced by osteoclasts activates Stat5 and leads to the suppression of bone resorption by inducing Dusp1 and Dusp2 expression, thus generating a cell-autonomous negative feedback loop in osteoclasts.

Published December 23, 2013

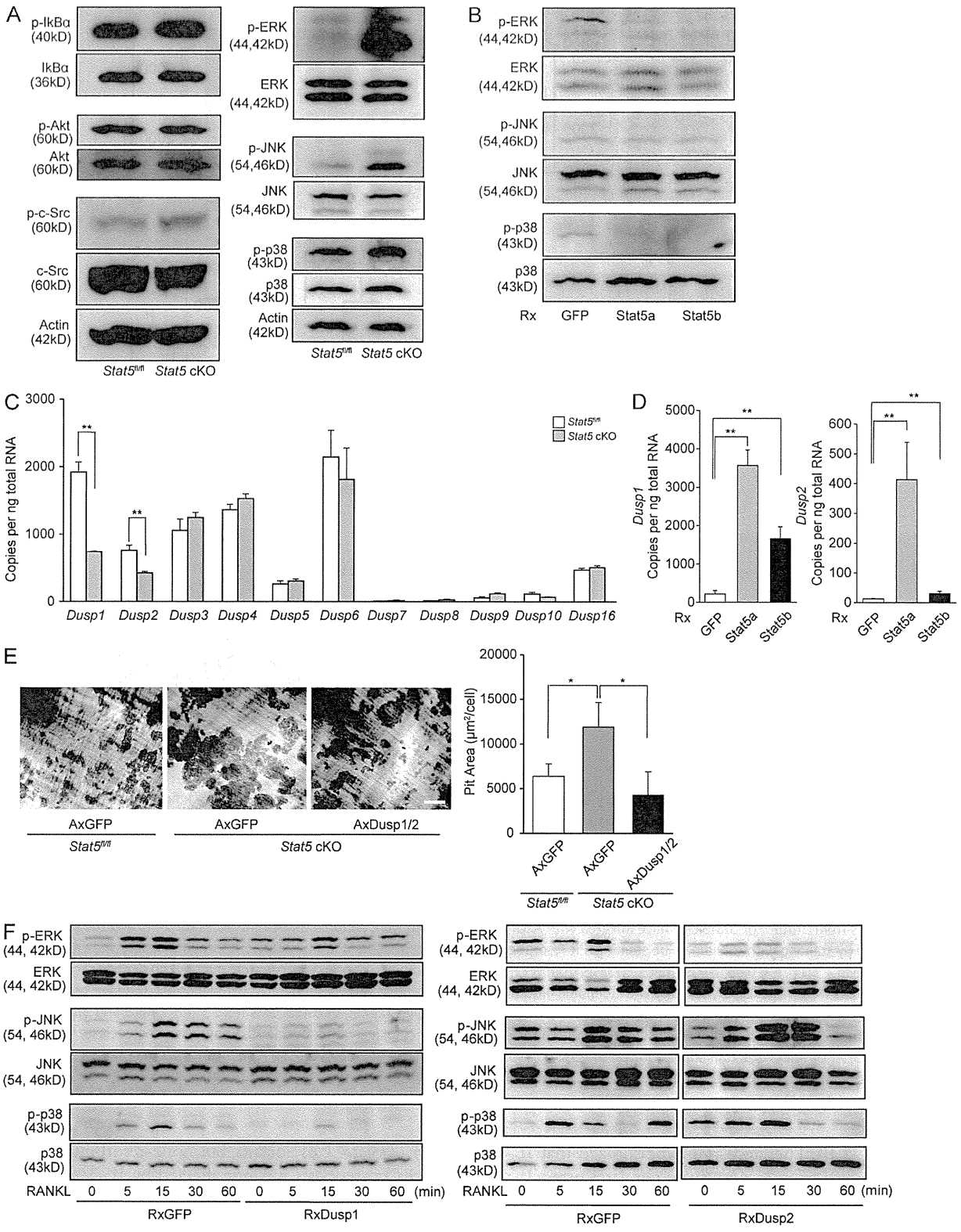

Figure 4. Stat5 negatively regulates the activity of MAPKs through the expression of Dusp1 and Dusp2. (A) Whole-cell lysates from *Stat5*$^{fl/fl}$ and *Stat5* cKO osteoclasts were subjected to Western blotting using antibodies against phospho-IκBα, phospho-Akt, phospho-c-Src, phospho-ERK1/2, phospho-JNK, and phopsho-p38. (B) Total cell lysates from WT osteoclasts retrovirally overexpressing Stat5a and Stat5b were analyzed by Western blotting using antibodies against phospho-ERK1/2, phospho-JNK, and phospho-p38. (C) Total RNA was extracted from *Stat5*$^{fl/fl}$ and *Stat5*

Published December 23, 2013

DISCUSSION

Multiple previous studies reported important roles for STAT family members in osteoclasts. Takayanagi et al. (2002) reported that β-interferon negatively regulates osteoclast differentiation through the Stat1 pathway, and Abu-Amer (2001) reported that IL-4 abrogates osteoclastogenesis through the Stat6 pathway. The present study demonstrated that Stat5 negatively regulates the bone-resorbing activity of osteoclasts, but it is not essential for their differentiation or survival. Stat family proteins have both redundant and nonredundant functions in many types of cells, and the loss of Stat5 may be compensated by other Stat family members or non-Stat proteins in the regulation of osteoclast differentiation and survival. IL-3, which is induced by RANKL, is a possible mediator of Stat5 activation in osteoclasts.

Stat5 cKO male mice exhibited significantly reduced bone mass at 8 wk of age, but female mice did not show significant difference. The cause of this sex difference is unclear, but Teglund et al. (1998) reported normal growth of Stat5b-deficient female mice. One possible explanation is that the Stat5 signaling pathway is somewhat different between males and females, although further investigation is needed. In an attempt to elucidate the mechanisms by which Stat5 suppresses the bone-resorbing activity of osteoclasts, we demonstrated that the activity of the MAPKs, in particular ERK, was increased in *Stat5* KO osteoclasts. Many previous studies have reported the role of ERK in osteoclasts. A recent study using $Erk1^{-/-}$ and $Erk2^{flox/flox}$ mice reported that Erk1 positively regulated osteoclast function (He et al., 2011), providing grounds for our proposal that the increased bone-resorbing activity of *Stat5* KO osteoclasts is, at least in part, caused by the increased activity of ERK. Although multiple studies have reported an antiapoptotic effect of ERK in osteoclasts (Miyazaki et al., 2000; Nakamura et al., 2003), we did not find an increased survival of *Stat5* KO osteoclasts. This discrepancy may be explained by the duration of ERK phosphorylation and its subcellular localization. Chen et al. (2005) demonstrated that both the duration of ERK activity and localization of ERK are important for the proper function of ERK. They concluded that the kinetics of ERK phosphorylation and the length of time that phospho-ERK is retained in the nucleus are responsible for the pro- versus antiapoptotic effect of ERK. Further studies are needed to precisely determine kinetic activity and localization of ERK in *Stat5* KO osteoclasts.

We speculated that the increased MAPK activity observed in Stat5 KO osteoclasts was caused by the absence of the proteins that are induced by Stat5 and affect the phosphorylation status of the MAPKs. As we anticipated, the expression of the MKPs *Dusp1* and *Dusp2* was reduced in *Stat5* cKO osteoclasts. Dusps are a heterogeneous group of protein phosphatases that dephosphorylate both phosphotyrosine and phosphoserine/phosphothreonine residues (Patterson et al., 2009). Some of the Dusp family members are known to serve as MKPs, which, as mentioned above, dephosphorylate MAPKs with substrate specificity. Carlson et al. (2009) reported that Dusp1 negatively regulates the bone-resorbing activity of osteoclasts, whereas the role of Dusp2 in osteoclasts at present remains elusive. Dusp1 is reported to dephosphorylate all of the MAPKs, whereas Dusp2 is induced mainly by ERK. Dusp2 is involved in the anchoring of ERK in the nucleus and suppresses ERK activation (Caunt et al., 2008). In accordance with these studies, the overexpression of Dusp2 in osteoclasts specifically reduced the activity of ERK among various MAPKs. Therefore, the increased MAPK activity in *Stat5* KO osteoclasts may be caused by the combined reduction of both *Dusp1* and *Dusp2*.

Among the various factors known to activate Stat5, IL-3 and GM-CSF induced the activation of Stat5 in osteoclasts. However, the duration of Stat5 activation by GM-CSF was much shorter than that by IL-3. Moreover, although IL-3 suppressed the osteoclast bone-resorbing activity, GM-CSF did not affect the bone resorption. Therefore, we speculated that IL-3 exerts a negative effect on bone resorption by Stat5 activation. IL-3 has been reported to suppress osteoclast differentiation by inhibiting the phosphorylation and degradation of IκB (Khapli et al., 2003) or by down-regulating c-Fms (Gupta et al., 2010). IL-3 is produced mainly by T cells after cell activation by antigens and mitogens, suggesting that the IL-3 secreted by activated T cells negatively regulates osteoclast function through the Stat5–Dusp axis. Interestingly, IL-3 expression was increased in osteoclasts in response to RANKL. Therefore, it is also possible that a cell-autonomous IL-3–Stat5–Dusp axis acts as a negative feedback loop in osteoclastic bone resorption. And therefore, IL-3 may have therapeutic potential in bone diseases such as osteoporosis and rheumatoid arthritis, in which osteoclast activity is increased.

A limitation of this study is that the IL-3 effect was assessed only in in vitro cultures of osteoclasts. Further studies are needed to determine whether IL-3 is also implicated in the activation of Stat5 in osteoclasts in vivo. In addition, we did not elucidate which genes regulated by Stat5 are directly responsible for increased activation of Stat5 cKO osteoclasts.

cKO osteoclasts, and the expression of *Dusp1*, *Dusp2*, *Dusp3*, *Dusp4*, *Dusp5*, *Dusp6*, *Dusp7*, *Dusp8*, *Dusp9*, *Dusp10*, and *Dusp16* was analyzed by quantitative real-time PCR. Data are represented as the mean ± SD (**, $P < 0.01$; $n = 3$). (D) Total RNA was prepared from osteoclasts retrovirally overexpressing GFP, Stat5a, or Stat5b, and the expression of *Dusp1* and *Dusp2* was analyzed by quantitative real-time PCR. Data are represented as the mean ± SD (**, $P < 0.01$; $n = 3$). (E) Bone-resorbing activity of $Stat5^{fl/fl}$ (AxGFP) and *Stat5* cKO osteoclasts adenovirally transfected with AxGFP and AxDusp1/2 was analyzed by pit formation assay. Representative resorption pits, visualized by toluidine blue staining, are also shown. Graph shows pit resorption area per osteoclast. Data are representative of three independent experiments (*, $P < 0.05$; $n = 3$). Bar, 100 µm. (F) Phosphorylation of ERK1/2, JNK, and p38 after RANKL stimulation in WT osteoclasts retrovirally overexpressing Dusp1 or Dusp2 was analyzed by Western blotting. Results are representative of two (A, B, E, and F) or three (C and D) independent experiments.

Published December 23, 2013

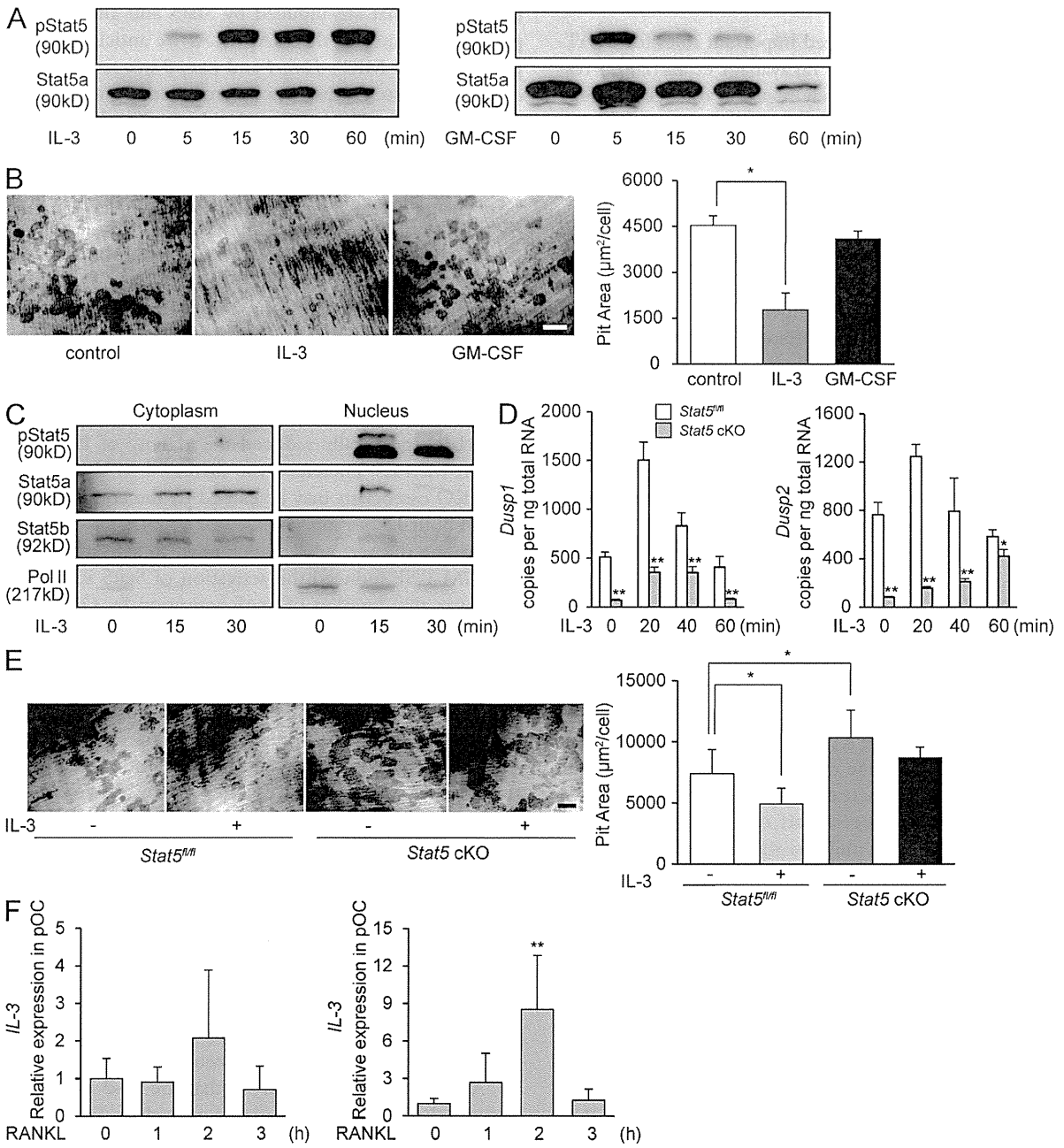

Figure 5. IL-3 may be a stimulator of Stat5 in osteoclasts. (A) WT osteoclasts were stimulated with IL-3 or GM-CSF, and whole-cell lysates were subjected to Western blotting using antibodies against phospho-Stat5 and Stat5a. (B) WT osteoclasts were cultured on dentin slices for 24 h with or without IL-3 and GM-CSF, and the resorption areas were visualized by toluidine blue staining and measured using an image analysis system. Representative resorption pits are shown (left). Graph shows pit resorption area per osteoclast (right). Data are represented as the mean ± SD (*, $P < 0.05$; $n = 3$). (C) Osteoclasts from WT mice were stimulated with IL-3 after serum starvation, and cytoplasmic and nuclear fractions were subjected to Western blotting using antibodies against phospho-Stat5, Stat5a, Stat5b, and RNA polymerase II. (D) Osteoclasts from *Stat5*$^{fl/fl}$ and *Stat5* cKO mice were stimulated with IL-3 after serum starvation, and total RNA was extracted. The expression of *Dusp1* (left) and *Dusp2* (right) was analyzed by quantitative real-time PCR. Data are represented as the mean ± SD (*, $P < 0.05$; **, $P < 0.01$; $n = 3$/group). (E) *Stat5*$^{fl/fl}$ or *Stat5* cKO osteoclasts were cultured on dentin slices for 24 h with or without IL-3, and the resorption areas were visualized by toluidine blue staining and measured using an image analysis system. Representative resorption pits are shown (left). Graph shows pit resorption area per osteoclast (right). Data are represented as the mean ± SD (*, $P < 0.05$). (B and E) Bars, 100 μm. (F) WT osteoclast precursors and osteoclasts were stimulated with RANKL for the indicated time, total RNA was prepared, and the expression of *IL-3* was analyzed by quantitative real-time PCR. Data are represented as the mean ± SD (**, $P < 0.01$ vs. 0 h; $n = 3$). Results in all panels are representative of two independent experiments.

Published December 23, 2013

Future studies are required to fully understand the mechanisms of transcriptional regulation of osteoclast function. In conclusion, we demonstrated that Stat5 negatively regulates the bone-resorbing function of osteoclasts by promoting *Dusp1* and *Dusp2* expression, and IL-3 appears to be one of the stimulators of stat5 in osteoclasts.

MATERIALS AND METHODS

Mice. *Stat5$^{fl/fl}$* mice, carrying the *Stat5a/b* gene with two loxP sequences were generated as previously described (Cui et al., 2004). The mice were on a C57BL/6 background. The presence of the floxed *Stat5* gene was determined by PCR around the 5′ loxP site using the primers 5′-GAAAGCATGAAAGGGTTGGAG-3′, 5′-AGCAGCAACCAGAGGACTAC-3′, and 5′-AAGTTATCTCGAGTTAGTCAGG-3′, giving a WT band of 450 bp and a floxed gene product of 200 bp. To generate *Stat5* cKO mice, we used cathepsin K–Cre mice (provided by S. Kato, Soma Chuo Hospital, Fukushima, Japan), in which the Cre recombinase gene is knocked into the *cathepsin K* locus and specifically expressed in osteoclasts (Nakamura et al., 2007). *Stat5* cKO mice and normal *Stat5$^{fl/fl}$* littermates were generated by mating *Cathepsin K–Cre$^{+/-}$ Stat5$^{fl/+}$* male mice with *Cathepsin K–Cre$^{-/-}$ Stat5$^{fl/fl}$* female mice. All animals were housed under specific pathogen–free conditions and treated with humane care under the approval of the Animal Care and Use Committee of the University of Tokyo.

Radiological analyses. Plain radiographs were taken using a soft x-ray apparatus (CMB-2; SOFTEX), and bone mineral density was measured by DXA using a bone mineral analyzer (PIXImus Densitometer; GE Healthcare). CT scanning of the distal femur was performed using Scan Xmate-L090 (Comscantecno) and was reconstructed into a 3D feature image with 3D-BON (RATOC Systems International).

Serum growth hormone, IGF-I, CTx-I, and osteocalcin measurement. Blood samples were collected retroorbitally under anesthesia, and serum was obtained using a BD Microtainer. Serum growth hormone was measured using a rat/mouse growth hormone ELISA (EMD Millipore). Serum IGF-I was measured using mouse/rat IGF-I Quantikine ELISA kit (R&D Systems). Serum CTx-I was measured using a RatLaps ELISA kit (Nordic Bioscience Diagnostic A/S). Serum osteocalcin was measured using a mouse osteocalcin EIA kit (Biomedical Technologies). Plasma was obtained using a BD Microtainer.

Histological analyses. Tissues were fixed in 4% paraformaldehyde/PBS, decalcified in 10% EDTA, embedded in paraffin, and cut into sections of 5-µm thickness. Hematoxylin and eosin (H&E) staining was performed according to the standard procedure. Histomorphometric analysis was performed on undecalcified sections from a point 0.15 mm below the growth plate to 0.6 mm of the primary spongiosa of the proximal tibia. For double labeling, mice were injected subcutaneously with 16 mg/kg body weight of calcein on days 4 and 1 before sacrifice. TRAP-positive cells were stained at pH 5.0 in the presence of L (+)–tartaric acid using naphthol AS-MX phosphate (Sigma-Aldrich) in *N,N*-dimethyl formamide as the substrate.

Generation of osteoclasts and survival/bone resorption assay. BM cells were obtained from the femur and tibia of 6-wk-old C57BL/6 mice, and BMDMs were cultured in α-MEM (Gibco) containing 10% FBS (Sigma-Aldrich) in the presence of 100 ng/ml M-CSF (R&D Systems) for 2 d. Osteoclasts were generated by stimulating BMDMs with 10 ng/ml M-CSF and 100 ng/ml RANKL (Wako Pure Chemical Industries, Ltd.) for an additional 4–5 d or by the co-culture system established by Takahashi et al. (1988). The survival assay was performed as follows. After osteoclasts were generated, both RANKL and M-CSF were removed from the culture (time 0), and osteoclasts were cultured for the indicated times. The survival rate of the cells was estimated as the percentage of morphologically intact TRAP$^+$ multinucleated cells compared with those at time 0. Actin ring formation was examined using rhodamine-phalloidin staining. In brief, cells were incubated for 30 min with rhodamine-conjugated phalloidin solution (Molecular Probes). The actin rings formed by osteoclasts were detected with a BZ-8100 fluorescence microscope (KEYENCE). The osteoclast bone resorption assays were performed as previously reported (Miyazaki et al., 2000). In brief, the cells were cultured on dentine slices for 24 h, and the resorption areas were visualized by staining with 1% toluidine blue and then measured using an image analysis system (MicroAnalyzer).

TUNEL staining. Cells undergoing apoptosis were identified by means of the TdT-mediated dUTP-digoxigenin nick-end labeling (TUNEL) method, which specifically labels the 3′-hydroxyl terminal of DNA strand breaks. The TUNEL staining procedure was performed using In Situ Cell Death Detection kit, Fluorescein (Roche), according to the manufacturer's recommendation. Apoptotic cells were recognized by fluorescence microscopy.

Expression constructs and gene transduction. For retrovirus construction, the full-length cDNA of the gene was amplified by PCR using KOD-plus (Takara Bio Inc.), subcloned into Zero Blunt TOPO II vectors (Invitrogen), and inserted into pMX-puro vectors (Kitamura, 1998). 2 × 10^6 BOSC23 packaging cells were transfected with 6 µg of the vectors using FuGENE 6 (Roche). 24 h later, the medium was replaced with fresh α-MEM/10% FBS, and cells were incubated for an additional 24 h. The supernatant was then collected as retroviral stock after centrifugation at 2,400 rpm for 3 min. 5× 10^6 BMDMs were incubated with 8 ml of retroviral stock for 5 h in the presence of 6 µg/ml polybrene and 30 ng/ml recombinant mouse M-CSF. After 5 h of retroviral infection, the medium was changed to α-MEM/10% FBS and 100 ng/ml M-CSF, and cells were cultured for an additional 24 h. BMDMs were recovered with trypsin, and puromycin-resistant cells were selected by incubation with α-MEM/10% FBS containing 2 µg/ml puromycin for 2 d and were then used for further experiments. The adenovirus GFP, Stat5a, Stat5b, Dusp1, Dusp2 expression vectors were synthesized using an Adeno-X expression system (Takara Bio Inc.). Viral titers were determined by the end point dilution assay, and the viruses were used at 50 MOI. Adenoviral infection of osteoclasts was performed as previously reported (Tanaka et al., 1998). In short, mouse co-cultures on days 5–6, when the osteoclasts began to appear, were incubated with a small amount of α-MEM containing the recombinant adenoviruses for 1 h at 37°C at the indicated MOI. The cells were washed twice with PBS and further incubated with α-MEM/10% FBS at 37°C. Experiments were performed 24 h after the infection was confirmed.

Real-time PCR analysis. Total RNA was extracted with ISOGEN (Wako Pure Chemical Industries, Ltd.), and a 1-µg aliquot was reverse transcribed using a QuantiTect Reverse Transcription kit (QIAGEN) to produce single-stranded cDNA. PCR was performed on an ABI Prism 7000 Sequence Detection System (Applied Biosystems) using QuantiTect SYBR Green PCR Master Mix (QIAGEN) according to the manufacturer's instructions. All reactions were performed in triplicate. After data collection, the mRNA copy number of a specific gene was calculated with a standard curve generated with serially diluted plasmids containing PCR amplicon sequences and then normalized to rodent total RNA with mouse β-actin serving as an internal control. Primer sequences were as follows: *β-actin* forward, 5′-AGATGTGGATCAGCAAGCA-3′; *β-actin* reverse, 5′-GCGCAAGTTAGGTTTTGTCA-3′; *Stat5a* forward, 5′-CCGAAACCTCTGGAATCTGA-3′; *Stat5a* reverse, 5′-ACGAACTCAGGGACCACTTG-3′; *Stat5b* forward, 5′-GTGAAGCCACAGATCAAGCA-3′; *Stat5b* reverse, 5′-TCGGTATCAAGGACGGAGTC-3′; *Nfatc1* forward, 5′-TCCGAGAATCGAGATCACCT-3′; *Nfatc1* reverse, 5′-AGGGGTCTCTGTAGGCTTCC-3′; *Ctsk* forward, 5′-GGACCCATCTCTGTGTCCAT-3′; *Ctsk* reverse, 5′-CCGAGCCAAGAGAGCATATC-3′; *Acp5* forward, 5′-CGTCTCTGCACAGATTGCAT-3′; *Acp5* reverse, 5′-AACTGCTTTTTGAGCCAGGA-3′; *Dusp1* forward, 5′-GAGCTGTGCAGCAAACAGTC-3′; *Dusp1* reverse, 5′-CTTCCGAGAAGCGTGATAGG-3′; *Dusp2* forward, 5′-ACTGTCCGGATCTGTGCTCT-3′; *Dusp2* reverse, 5′-CAGCTGGCAGAGACATTGAG-3′;

Published December 23, 2013

Dusp3 forward, 5′-TTGAAAGGGCCACAGATTTC-3′; *Dusp3* reverse, 5′-AGTTTCACCTTGCCCTCCTT-3′; *Dusp4* forward, 5′-CTGTACCTCCCAGCACCAAT-3′; *Dusp4* reverse, 5′-GACGGGGATGCACTTGTACT-3′; *Dusp5* forward, 5′-TGCACCACCCACCTACACTA-3′; *Dusp5* reverse, 5′-AGGACCTTGCCTCCTTCTTC-3′; *Dusp6* forward, 5′-TTGAATGTCACCCCCAATTT-3′; *Dusp6* reverse, 5′-CATCGTTCATGGACAGGTTG-3′; *Dusp7* forward, 5′-TGCCAAGGACTCTACCAACC-3′; *Dusp7* reverse, 5′-GAGAGGTTCTGGCTCCAGTG-3′; *Dusp8* forward, 5′-GTCCATGAGCCTCTCTCAGC-3′; *Dusp8* reverse, 5′-TGAAACGGCTCTCACAGATG-3′; *Dusp9* forward, 5′-ACCTTGAGCTGTGGCCTAGA-3′; *Dusp9* reverse, 5′-GGGGATCTGCTTGTAGTGGA-3′; *Dusp10* forward, 5′-GCGGCAGTACTTTGAAGAGG-3′; *Dusp10* reverse, 5′-AGGTTCGGGGAAATAATTGG-3′; *Dusp16* forward, 5′-CAGCGAGATGTCCTCAACAA-3′; *Dusp16* reverse, 5′-TAAGCACACAGCCATTGGAG-3′; *IL-3* forward, 5′-CTGCCTACATCTGCGAATGA-3′; *IL-3* reverse, and 5′-TTAGGAGAGACGGAGCCAGA-3′.

Western blotting. Cells were washed with ice-cold PBS, and proteins were extracted at 4°C with M-PER, an inhibitor cocktail. Equivalent amounts of protein were subjected to SDS-PAGE with 7.5–15% Tris-Glycin gradient gel or 15% Tris-Glycin gel and transferred onto PVDF membranes (Bio-Rad Laboratories, Inc.). After blocking with 6% milk/TBS-T, membranes were incubated with primary antibodies to Stat5a, Stat5b, RNA polymerase (Santa Cruz Biotechnology, Inc.), Cre recombinase (Covance), phospho-Stat5, cleaved caspase-3, ERK1/2, phospho-ERK1/2, JNK, phospho-JNK, p38, phospho-p38, phospho-Akt, Akt, phospho-IκB, IκB, phospho–c-Src (Cell Signaling Technology), c-Src (EMD Millipore), and β-actin (Sigma-Aldrich), followed by HRP-conjugated goat anti–mouse IgG and goat anti–rabbit IgG (Promega). Immunoreactive bands were visualized with ECL (GE Healthcare) according to the manufacturer's instructions. The blots were stripped by incubating for 20 min in stripping buffer (2% SDS, 100 mM 2-mercaptoethanol, and 62.5 mM Tris-HCl, pH 6.7) at 50°C and then were reprobed with other antibodies.

Microarray analysis. BM cells were isolated from *Stat5*$^{fl/fl}$ and *Stat5* cKO mice. Osteoclasts were generated from these cells by culture with M-CSF plus RANKL. Total RNA was extracted and microarray analysis was undertaken using the Mouse Oligo chip 24K (TORAY). Data were analyzed using a 3D-Gene Scanner 3000 (TORAY) and deposited in Minimum Information about a Microarray Experiment compliant in Gene Expression Omnibus (GEO accession no. GSE51283).

Data analysis. Data are presented as the means ± SD. Statistical analyses were performed by two-tailed unpaired Student's *t* test. The value of $P < 0.05$ was considered significant.

We thank R. Yamaguchi and H. Kawahara (The University of Tokyo, Bunkyo-ku, Tokyo, Japan) for providing expert technical assistance. Shigeaki Kato provided us with cathepsin K–Cre mice.

This work was supported in part by Grants-in-Aid from the Ministry of Education, Culture, Sports, Science and Technology of Japan. The research of L. Hennighausen was funded through the Intramural Program of the National Institute of Diabetes and Digestive and Kidney Diseases, National Institutes of Health.

Pacific Edit reviewed the manuscript before submission.

The authors have no conflicting financial interests.

Submitted: 14 March 2013
Accepted: 26 November 2013

REFERENCES

Abu-Amer, Y. 2001. IL-4 abrogates osteoclastogenesis through STAT6-dependent inhibition of NF-kappaB. *J. Clin. Invest.* 107:1375–1385. http://dx.doi.org/10.1172/JCI10530

Akira, S. 1999. Functional roles of STAT family proteins: lessons from knockout mice. *Stem Cells.* 17:138–146. http://dx.doi.org/10.1002/stem.170138

Baron, R. 1989. Molecular mechanisms of bone resorption by the osteoclast. *Anat. Rec.* 224:317–324. http://dx.doi.org/10.1002/ar.1092240220

Carlson, J., W.G. Cui, Q. Zhang, X.Q. Xu, F. Mercan, A.M. Bennett, and A. Vignery. 2009. Role of MKP-1 in osteoclasts and bone homeostasis. *Am. J. Pathol.* 175:1564–1573. http://dx.doi.org/10.2353/ajpath.2009.090035

Caunt, C.J., C.A. Rivers, B.L. Conway-Campbell, M.R. Norman, and C.A. McArdle. 2008. Epidermal growth factor receptor and protein kinase C signaling to ERK2: spatiotemporal regulation of ERK2 by dual specificity phosphatases. *J. Biol. Chem.* 283:6241–6252. http://dx.doi.org/10.1074/jbc.M706624200

Chen, J.R., L.I. Plotkin, J.I. Aguirre, L. Han, R.L. Jilka, S. Kousteni, T. Bellido, and S.C. Manolagas. 2005. Transient versus sustained phosphorylation and nuclear accumulation of ERKs underlie anti-versus pro-apoptotic effects of estrogens. *J. Biol. Chem.* 280:4632–4638. http://dx.doi.org/10.1074/jbc.M411530200

Cui, Y., G. Riedlinger, K. Miyoshi, W. Tang, C. Li, C.X. Deng, G.W. Robinson, and L. Hennighausen. 2004. Inactivation of Stat5 in mouse mammary epithelium during pregnancy reveals distinct functions in cell proliferation, survival, and differentiation. *Mol. Cell. Biol.* 24:8037–8047. http://dx.doi.org/10.1128/MCB.24.18.8037-8047.2004

Gupta, N., A.P. Barhanpurkar, G.B. Tomar, R.K. Srivastava, S. Kour, S.T. Pote, G.C. Mishra, and M.R. Wani. 2010. IL-3 inhibits human osteoclastogenesis and bone resorption through downregulation of c-Fms and diverts the cells to dendritic cell lineage. *J. Immunol.* 185:2261–2272. http://dx.doi.org/10.4049/jimmunol.1000015

He, Y.Z., K. Staser, S.D. Rhodes, Y.L. Liu, X.H. Wu, S.J. Park, J. Yuan, X.L. Yang, X.H. Li, L. Jiang, et al. 2011. Erk1 positively regulates osteoclast differentiation and bone resorptive activity. *PLoS ONE.* 6:e24780. http://dx.doi.org/10.1371/journal.pone.0024780

Hennighausen, L., and G.W. Robinson. 2008. Interpretation of cytokine signaling through the transcription factors STAT5A and STAT5B. *Genes Dev.* 22:711–721. http://dx.doi.org/10.1101/gad.1643908

Hoelbl, A., B. Kovacic, M.A. Kerenyi, O. Simma, W. Warsch, Y.Z. Cui, H. Beug, L. Hennighausen, R. Moriggl, and V. Sexl. 2006. Clarifying the role of Stat5 in lymphoid development and Abelson-induced transformation. *Blood.* 107:4898–4906. http://dx.doi.org/10.1182/blood-2005-09-3596

Ilaria, R.L. Jr., and R.A. Van Etten. 1996. P210 and P190(BCR/ABL) induce the tyrosine phosphorylation and DNA binding activity of multiple specific STAT family members. *J. Biol. Chem.* 271:31704–31710. http://dx.doi.org/10.1074/jbc.271.49.31704

Karsenty, G., and E.F. Wagner. 2002. Reaching a genetic and molecular understanding of skeletal development. *Dev. Cell.* 2:389–406. http://dx.doi.org/10.1016/S1534-5807(02)00157-0

Khapli, S.M., L.S. Mangashetti, S.D. Yogesha, and M.R. Wani. 2003. IL-3 acts directly on osteoclast precursors and irreversibly inhibits receptor activator of NF-kappa B ligand-induced osteoclast differentiation by diverting the cells to macrophage lineage. *J. Immunol.* 171:142–151.

Kitamura, T. 1998. New experimental approaches in retrovirus-mediated expression screening. *Int. J. Hematol.* 67:351–359. http://dx.doi.org/10.1016/S0925-5710(98)00025-5

Lacey, D.L., E. Timms, H.L. Tan, M.J. Kelley, C.R. Dunstan, T. Burgess, R. Elliott, A. Colombero, G. Elliott, S. Scully, et al. 1998. Osteoprotegerin ligand is a cytokine that regulates osteoclast differentiation and activation. *Cell.* 93:165–176. http://dx.doi.org/10.1016/S0092-8674(00)81569-X

Miyazaki, T., H. Katagiri, Y. Kanegae, H. Takayanagi, Y. Sawada, A. Yamamoto, M.P. Pando, T. Asano, I.M. Verma, H. Oda, et al. 2000. Reciprocal role of ERK and NF-κB pathways in survival and activation of osteoclasts. *J. Cell Biol.* 148:333–342. http://dx.doi.org/10.1083/jcb.148.2.333

Nakamura, H., A. Hirata, T. Tsuji, and T. Yamamoto. 2003. Role of osteoclast extracellular signal-regulated kinase (ERK) in cell survival and maintenance of cell polarity. *J. Bone Miner. Res.* 18:1198–1205. http://dx.doi.org/10.1359/jbmr.2003.18.7.1198

Nakamura, T., Y. Imai, T. Matsumoto, S. Sato, K. Takeuchi, K. Igarashi, Y. Harada, Y. Azuma, A. Krust, Y. Yamamoto, et al. 2007. Estrogen prevents bone loss via estrogen receptor alpha and induction of Fas ligand in osteoclasts. *Cell.* 130:811–823. http://dx.doi.org/10.1016/j.cell.2007.07.025

Published December 23, 2013

Patterson, K.I., T. Brummer, P.M. O'Brien, and R.J. Daly. 2009. Dual-specificity phosphatases: critical regulators with diverse cellular targets. *Biochem. J.* 418:475–489.

Roodman, G.D. 2004. Mechanisms of bone metastasis. *Discov. Med.* 4:144–148.

Seeman, E. 2003. Reduced bone formation and increased bone resorption: rational targets for the treatment of osteoporosis. *Osteoporos. Int.* 14:S2–S8. http://dx.doi.org/10.1007/s00198-002-1340-9

Sommer, B., R. Felix, C. Sprecher, M. Leunig, R. Ganz, and W. Hofstetter. 2005. Wear particles and surface topographies are modulators of osteoclastogenesis in vitro. *J. Biomed. Mater. Res. A.* 72A:67–76. http://dx.doi.org/10.1002/jbm.a.30202

Suda, T., N. Takahashi, N. Udagawa, E. Jimi, M.T. Gillespie, and T.J. Martin. 1999. Modulation of osteoclast differentiation and function by the new members of the tumor necrosis factor receptor and ligand families. *Endocr. Rev.* 20:345–357. http://dx.doi.org/10.1210/er.20.3.345

Takahashi, N., T. Akatsu, N. Udagawa, T. Sasaki, A. Yamaguchi, J.M. Moseley, T.J. Martin, and T. Suda. 1988. Osteoblastic cells are involved in osteoclast formation. *Endocrinology.* 123:2600–2602. http://dx.doi.org/10.1210/endo-123-5-2600

Takayanagi, H., H. Iizuka, T. Juji, T. Nakagawa, A. Yamamoto, T. Miyazaki, Y. Koshihara, H. Oda, K. Nakamura, and S. Tanaka. 2000. Involvement of receptor activator of nuclear factor kappaB ligand/osteoclast differentiation factor in osteoclastogenesis from synoviocytes in rheumatoid arthritis. *Arthritis Rheum.* 43:259–269. http://dx.doi.org/10.1002/1529-0131(200002)43:2<259::AID-ANR4>3.0.CO;2-W

Takayanagi, H., S. Kim, K. Matsuo, H. Suzuki, T. Suzuki, K. Sato, T. Yokochi, H. Oda, K. Nakamura, N. Ida, et al. 2002. RANKL maintains bone homeostasis through c-Fos-dependent induction of interferon-beta. *Nature.* 416:744–749. http://dx.doi.org/10.1038/416744a

Tanaka, S. 2007. Signaling axis in osteoclast biology and therapeutic targeting in the RANKL/RANK/OPG system. *Am. J. Nephrol.* 27:466–478. http://dx.doi.org/10.1159/000106484

Tanaka, S., T. Takahashi, H. Takayanagi, T. Miyazaki, H. Oda, K. Nakamura, H. Hirai, and T. Kurokawa. 1998. Modulation of osteoclast function by adenovirus vector-induced epidermal growth factor receptor. *J. Bone Miner. Res.* 13:1714–1720. http://dx.doi.org/10.1359/jbmr.1998.13.11.1714

Teglund, S., C. McKay, E. Schuetz, J.M. van Deursen, D. Stravopodis, D. Wang, M. Brown, S. Bodner, G. Grosveld, and J.N. Ihle. 1998. Stat5a and Stat5b proteins have essential and nonessential, or redundant, roles in cytokine responses. *Cell.* 93:841–850. http://dx.doi.org/10.1016/S0092-8674(00)81444-0

Van Etten, R.A. 2007. Aberrant cytokine signaling in leukemia. *Oncogene.* 26:6738–6749. http://dx.doi.org/10.1038/sj.onc.1210758

Villa, A., M.M. Guerrini, B. Cassani, A. Pangrazio, and C. Sobacchi. 2009. Infantile malignant, autosomal recessive osteopetrosis: the rich and the poor. *Calcif. Tissue Int.* 84:1–12. http://dx.doi.org/10.1007/s00223-008-9196-4

Wakao, H., F. Gouilleux, and B. Groner. 1994. Mammary gland factor (MGF) is a novel member of the cytokine regulated transcription factor gene family and confers the prolactin response. *EMBO J.* 13:2182–2191.

Yao, Z., Y. Cui, W.T. Watford, J.H. Bream, K. Yamaoka, B.D. Hissong, D. Li, S.K. Durum, Q. Jiang, A. Bhandoola, et al. 2006. Stat5a/b are essential for normal lymphoid development and differentiation. *Proc. Natl. Acad. Sci. USA.* 103:1000–1005. http://dx.doi.org/10.1073/pnas.0507350103

Yasuda, H., N. Shima, N. Nakagawa, K. Yamaguchi, M. Kinosaki, S. Mochizuki, A. Tomoyasu, K. Yano, M. Goto, A. Murakami, et al. 1998. Osteoclast differentiation factor is a ligand for osteoprotegerin/osteoclastogenesis-inhibitory factor and is identical to TRANCE/RANKL. *Proc. Natl. Acad. Sci. USA.* 95:3597–3602. http://dx.doi.org/10.1073/pnas.95.7.3597

The Journal of Foot & Ankle Surgery 53 (2014) 41–46

Contents lists available at ScienceDirect

The Journal of Foot & Ankle Surgery

journal homepage: www.jfas.org

Midterm Results of Resection Arthroplasty for Forefoot Deformities in Patients with Rheumatoid Arthritis and the Risk Factors Associated with Patient Dissatisfaction

Takumi Matsumoto, MD, PhD [1], Yuho Kadono, MD, PhD [1], Jinju Nishino, MD [2], Kozo Nakamura, MD, PhD [1], Sakae Tanaka, MD, PhD [1], Tetsuro Yasui, MD, PhD [1]

[1] *Department of Orthopaedic Surgery, Faculty of Medicine, University of Tokyo, Bunkyo-ku, Tokyo, Japan*
[2] *Department of Orthopaedics and Rheumatology, Nishino Clinic, Kita-ku, Tokyo, Japan*

ARTICLE INFO

Level of Clinical Evidence: 4

Keywords:
forefoot surgery
hammer toe
Hoffmann procedure
outcome
panmetatarsal

ABSTRACT

We investigated the midterm results of resection arthroplasty of all 5 metatarsal heads in patients with rheumatoid arthritis and forefoot deformity and analyzed the factors that affect patient satisfaction levels. Of 64 patients (1 male, 63 females), 107 feet were treated with resection arthroplasty for forefoot deformity at our hospital from January 1992 to December 2005. The mean follow-up period was 5.8 ± 3.1 years, with all patients having at least 1 year of follow-up. Of the 64 patients, 75% were satisfied with the surgery. The mean score for the postoperative Japanese Society for Surgery of the Foot lesser metatarsophalangeal-interphalangeal scale was 75.0 ± 15.8 points. Multivariate logistic regression analysis showed that patient-reported dissatisfaction was significantly associated with the recurrence of hammer toe deformity (odds ratio 2.66, 95% confidence interval 1.07 to 6.97), shortening of the resection arthroplasty space (odds ratio 0.85 for a 1-unit increase, 95% confidence interval 0.74 to 0.96), and the recurrence of hallux valgus (odds ratio 1.04 for a 1-unit increase, 95% confidence interval 1.00 to 1.09) during the postoperative period. From our results, interventions to prevent recurrence of hammer toe deformity, especially in toes with preoperative metatarsophalangeal joint dislocations, have been shown to be important in preventing complications and patient dissatisfaction after resection arthroplasty.

Foot involvement, a major feature of rheumatoid arthritis (RA), has a profound influence on the mobility and functional capacity of patients with RA (1). Forefoot deformity is characterized by typical changes, such as hallux valgus, subluxation or dislocation of the lesser toes at the metatarsophalangeal joints (MTPJs), and hammer toe deformity of the lesser toes (2). Approximately 40% to 80% of patients with RA will experience forefoot deformity, which severely affects their quality of life (3,4). Resection arthroplasty for forefoot deformity was pioneered by Hoffmann (5) in 1912, and various modifications have been made by a number of surgeons (6,7,8,9,10,11,12,13). Although several attempts to preserve the MTPJs have been reported (14,15,16,17), resection arthroplasty is still a quite valuable procedure for patients with RA because of its high success rate and the simplicity of the procedure. However, controversy exists regarding to how to manage the first metatarsal, with resection (6,18,19,20), arthrodesis (21,22,23), or silicone arthroplasty (24,25) touted as appropriate methods. Although the results of resection arthroplasty for all 5 metatarsals have generally been satisfactory, complications associated with the procedure have been reported, including recurrence of hallux valgus (26,27,28), hammer toe deformity, painful callosities (29), and the development of osteophytes at the stump of the metatarsal (7,12). Furthermore, it remains unclear the extent to which these factors affect patient satisfaction levels.

Patients and Methods

Study Design and Aims

The purpose of the present retrospective, observational study was to clarify the risk factors associated with unsatisfactory results after resection arthroplasty of all 5 metatarsal heads in a group of patients with RA and painful forefoot deformities that included hammer toes with MTPJ subluxations. The research ethics committees of the University of Tokyo (Tokyo, Japan) approved the present investigation.

Patients

From January 1992 to December 2005, 86 patients (148 feet) with severe painful deformity of the forefoot caused by RA underwent resection arthroplasty of the MTPJs (excision of the metatarsal heads). We identified the patients eligible for inclusion by reviewing the database for RA at our department. Of these, 22 patients had died or could not be located before the follow-up examination. Therefore, 64 patients (107 feet, 535 rays [metatarsal and corresponding toe]) were studied at the follow-up examination in 2006. The demographic information of the included patients is listed in

Financial Disclosure: None reported.
Conflict of Interest: None reported.
Address correspondence to: Tetsuro Yasui, MD, PhD, Department of Orthopaedic Surgery, University of Tokyo Faculty of Medicine, 7-3-1 Hongo, Bunkyo-ku, Tokyo 113-0033, Japan.
E-mail address: YASUIT-ORT@h.u-tokyo.ac.jp (T. Yasui).

1067-2516/$ - see front matter © 2014 by the American College of Foot and Ankle Surgeons. All rights reserved.
http://dx.doi.org/10.1053/j.jfas.2013.09.014

Table 1
Patient demographics

Variable	Value
Patients; feet (n)	64; 107
Gender; feet (n)	
Male	1; 1
Female	63; 106
Age (y)	61.0 ± 10.0
Disease duration at surgery (y)	19.9 ± 8.7
Follow-up duration (y)	5.8 ± 3.1
Preoperative HV angle (°)	41.4 ± 16.4
Preoperative dislocated MTPJ at each lesser toe (n)	
II	81 (76)
III	92 (86)
IV	66 (62)
V	30 (28)

Abbreviations: HV, hallux valgus; MTPJ, metatarsophalangeal joint.
Data presented as mean ± standard deviation or n (%).

Table 1. The patients included 1 male (1.56%; 1 foot [0.93%]) and 63 females (98.44%; 106 feet [99.07%]). Their mean age was 61.0 ± 10.0 years.

The mean follow-up duration was 5.8 ± 3.1 years. The mean RA duration at surgery was 19.9 ± 8.7 years. The mean preoperative hallux valgus angle was 41.4° ± 16.4°. Preoperatively, 97 of the 107 feet (90.7%) had more than 1 dislocated MTPJ involving the lesser toes. The frequency of a dislocated MTPJ at each lesser toe was 76% (81 of 107) for the second ray, 86% (92 of 107) for the third, 62% (66 of 107) for the fourth, and 28% (30 of 107) for the fifth.

Surgical Procedure

All patients were treated using the method of Hoffmann (5), which consisted of resection of all 5 metatarsal heads, including that of the hallux and the 4 lesser rays. We used 3 longitudinal dorsal incisions, instead of the single plantar incision used by Hoffmann (5). Resection was performed to form a smooth curve by planning for the first and second toes to be of equal length, with the length of the other toes tapering gently from the second through to the fifth (Fig. 1). In 1 case, in which an adequate excision space was not gained by metatarsal head resection, the base of the phalange was also excised to avoid unnecessary shortening of the metatarsals. Flexion contractures of the proximal and, sometimes, distal, interphalangeal joints were corrected by closed manipulation without sectioning the tendons or capsules. All toes and metatarsals were temporarily stabilized using longitudinally positioned Kirschner wires (K-wires) that extended percutaneously from the toe tip, across the metatarsal head resection cleft, and into the shaft of the corresponding metatarsal. Patients were allowed to bear weight as tolerated on the heel, using a heel weightbearing shoe. The K-wires were removed 3 weeks after surgery. The operations were performed by 13 attending surgeons.

Clinical Assessment

At the follow-up examination in 2006, the patients were asked to complete a questionnaire for each operated foot. The questionnaire was handed out by a nurse at the outpatient clinic. The patients were asked to rate their overall satisfaction at that point using a 4-point Likert scale (excellent, good, fair, or poor) and asked whether they would undergo the same surgery again with their current knowledge of the procedure and outcomes. If not completely satisfied, the patients were also asked to provide reasons for their dissatisfaction (multiple answers were allowed, including pain, deformity [any subjective abnormal appearance about the toes, including hallux valgus and hammer toe], footwear requirement, and other). The clinical outcome was evaluated using the Japanese Society for Surgery of the Foot lesser metatarsophalangeal-interphalangeal scale (JSSF lesser scale), which ranges from 0 to 100 points and includes 3 major items: pain (40 points), function (45 points), and alignment (15 points) (30,31). Patients were also clinically evaluated for hammer toe deformities and callosities. An independent board-certified member of the Japanese Orthopedic Association who was not otherwise involved in the present study performed these clinical assessments at the outpatient clinic.

Radiographic Evaluation

The hallux valgus angle was measured as the angle between the longitudinal axis of the first metatarsal and the longitudinal axis of the proximal phalanx as viewed on the standing anteroposterior radiograph projection, before surgery and at the final follow-up visit (32). MTPJ dislocations were noted from the preoperative radiographs and defined as a condition characterized by complete overlapping of the proximal phalanx base and metatarsal head as viewed on the standing anteroposterior radiograph. The excision arthroplasty space was measured immediately after K-wire removal and at the follow-up visit in 2006 and was defined as the minimum distance from the intersection point between the longitudinal axis and the proximal end of the proximal phalanx to the distal margin of the stump of the corresponding metatarsal (Fig. 2). The space occupied by the formation of osteophytes (referred to as "size of osteophytes") at the metatarsal stump was measured at the final follow-up on the standard weightbearing anteroposterior radiograph by drawing a perpendicular line from the most prominent point of the osteophytes to a tangential line along the medial or lateral cortex of the metatarsal. The length of this perpendicular line was measured, and the sum of the medial and lateral lines was defined as the "size of osteophytes" at the stump (Fig. 2). All the radiographic evaluations were digitally measured using Picture Archiving and Communication System software (SYNAPSE, Fujifilm Medical, Tokyo, Japan). To remove the influence of interobserver variability, all measurements were taken by an independent board-certified member of the Japanese Orthopedic Association who was not otherwise involved in the present study. To determine the precision of measurements,

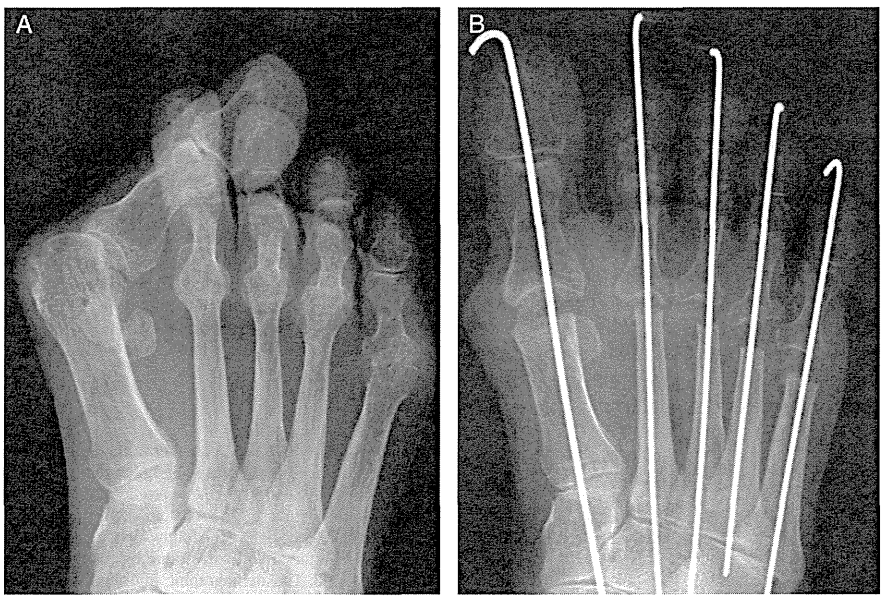

Fig. 1. (*A*) Standing preoperative anteroposterior radiograph. (*B*) Standing anteroposterior radiograph of the same foot immediately postoperatively with resection of all 5 metatarsal heads.

Fig. 2. Measurement of the excision arthroplasty space and size of the osteophytes at the metatarsal stump. The excision arthroplasty space was defined as a minimum distance (c) from the intersection point between longitudinal axis and the proximal end of the proximal phalanx to the stump of the metatarsal bone. A perpendicular line was drawn from the most prominent point of the osteophyte to a tangential line running along the medial or lateral cortex of the metatarsal bone. The osteophyte size was defined as the sum of the length of the medial (a) and lateral (b) perpendicular lines.

the intraclass correlation coefficient and the standard error of measurement were calculated from the evaluation data, which were collected from 35 randomly selected films using a random number generator software program, and graded by the observer, who was unaware of the patients' identity, 2 times at an interval of at least 6 months. The intraclass correlation coefficient for the hallux valgus angle, resection arthroplasty space, and size of the osteophytes was 0.99 (95% confidence interval [CI] 0.98 to 1.00), 0.96 (95% CI 0.91 to 0.98), and 0.99 (95% CI 0.98 to 1.00), respectively. The standard error of measurement for the hallux valgus angle, resection arthroplasty space, and size of the osteophytes was 1.16° (95% CI 0.90° to 1.62°), 0.49 mm (95% CI 0.38 to 0.68), and 0.85 mm (95% CI 0.67 to 1.2), respectively. These results indicated good reproducibility and validity of the measurements.

Statistical Analysis

Paired Student's *t* tests were used to assess the changes in the hallux valgus angles, and unpaired *t* tests were used to analyze the radiographic measurements and total scores for the JSSF lesser scale. On multivariate logistic regression analysis, all variables with $p < .5$ on univariate analysis were entered into the model, with the exception of the JSSF lesser scale. The chi-square test and Fisher's exact test were used to analyze the variables, including preoperative MTPJ dislocation, hammer toe recurrence, and painful callosities. All data are reported as the mean ± standard deviation. For each statistical analysis, $p \leq .05$ was considered statistically significant. Statistical analyses of the data were performed using the statistical software program JMP9 (SAS Institute, Cary, NC).

Results

The results of the self-reported questionnaire showed that patients rated the results of the surgery as excellent in 31 (29%) of the 107 feet, good in 41 (38%), fair in 16 (15%), and poor in 19 (18%). The reason for the dissatisfaction was pain in 39 feet (36%), deformity in 25 (23%), footwear requirements in 10 (9%), and other in 6 (6%; Table 2). Of the 64 patients, 75% stated that they would undergo the same procedure again if their symptoms warranted it. To determine the factors that influenced these results, the satisfaction ratings were divided into satisfactory and unsatisfactory groups (i.e., those with excellent or good results [satisfactory, n = 72 feet] and those with fair or poor results [unsatisfactory, n = 35 feet]). The mean JSSF lesser scale at the final follow-up visit was 75.0 points (range 52 to 97), with a statistically significant difference observed between the satisfactory and unsatisfactory groups (80.6 ± 11.1 vs 63.0 ± 17.5, respectively; $p < .001$; Table 3). No statistically significant difference was found in the disease duration or duration of the observation period between the 2 groups ($p = .367$ and $p = .331$, respectively; Table 3).

Table 2
Results of self-reported questionnaire (n = 107 feet in 64 patients)

Patient Satisfaction Level	Feet (n)
Satisfactory group	
Excellent	31 (29)
Good	41 (38)
Unsatisfactory group	
Fair	16 (15)
Poor	19 (17)
Reason for dissatisfaction*	
Pain	39 (36)
Deformity	25 (23)
Footwear	10 (9)
Other	6 (6)
Total feet overall	107 (100)

Data in parentheses are percentages.
* Multiple answers were allowed for queries regarding reason for dissatisfaction.

The mean hallux valgus angle at the final follow-up visit was 19.2° ± 11.7°, significantly lower statistically than the preoperative angle of 41.4° ± 16.4° ($p < .001$). No statistically significant difference in the preoperative hallux valgus angle was observed between the satisfied and unsatisfied groups (41.1° ± 17.9° vs 42.1° ± 12.3°, respectively; $p = .757$). Although the mean hallux valgus angle at the final follow-up visit was greater in the unsatisfied group than in the satisfied group, this difference was not statistically significant (17.9° ± 12.1° vs 22.2° ± 10.3°, respectively; $p = .077$; Table 3).

The mean distance between the stump of the resected metatarsal and the base of the proximal phalanx (resection arthroplasty space) immediately after K-wire removal was 2.6 mm for the first, 2.1 mm for the second, 2.6 mm for the third, 4.6 mm for the fourth, and 4.7 mm for the fifth, with the sum of all MTPJs equaling 16.6 ± 9.9 mm (Table 3). At the final follow-up visit, these distances had decreased to 1.4, 1.3, 1.0, 1.2, and 1.4 mm for the first, second, third, fourth, and fifth, respectively, with a sum of 6.3 ± 4.5 mm (Table 3). No statistically significant difference was found in the excision space distance immediately after K-wire removal between the satisfied and unsatisfied groups ($p = .838$). However, at the final follow-up visit, the unsatisfied group exhibited smaller distances at all MTPJs than those in the satisfied group, with statistically significant differences observed between the 2 groups at the second and fifth MTPJ joints (1.5 ± 1.3 mm vs 0.8 ± 1.0 mm, $p = .009$; and 1.6 ± 1.5 mm vs 1.0 ± 1.2 mm, $p = .045$, respectively). These differences also led to a significant difference in the sum of all MTPJs between the 2 groups (satisfied group 6.9 ± 4.6 mm vs unsatisfied group 5.0 ± 3.9 mm, $p = .042$; Table 3).

The mean size of the osteophytes observed at the metatarsal stumps was 3.7, 3.5, 2.6, 1.4, and 0.8 mm at the first, second, third, fourth, and fifth, with a sum of all MTPJs of 12.3 ± 7.1 mm. No statistically significant difference was found in the size of the osteophytes between the satisfied and unsatisfied groups (11.9 ± 7.1 mm vs 13.0 ± 7.1 mm, respectively; $p = .485$; Table 3).

At the final follow-up visit, hammer toe recurrence was observed in 113 of the 428 lesser toes (rays) (26%) that underwent surgery. Of the 107 feet, 49 (46%) had more than 1 recurrent hammer toe at the final follow-up visit, and this prevalence was significantly different between the satisfied and unsatisfied groups (41% vs 58%, respectively; $p = .018$). The frequency of hammer toe recurrence at the second to fifth toes was 29% (31 of 107), 31% (33 of 107), 22% (24 of 107), and 23% (25 of 107), with a relatively high frequency of recurrence at the second and third toes compared with the other toes (Table 3); however, this difference was not significantly different.

A multivariate logistic regression analysis was performed to identify the independent factors associated with the development of an unsatisfactory result (Table 4). Patients with recurrent hammer

Table 3
Prevalence of risk factors stratified by outcome (n = 107 feet in 64 patients)

Variable	Total (n = 107 feet)	Satisfactory (n = 72 feet)	Unsatisfactory (n = 35 feet)	*p* Value
Observation period (mo)	59.9 ± 38.3	63.0 ± 41.0	55.3 ± 29.0	.331
Duration of disease (y)	19.9 ± 8.8	19.4±8.8	21.0 ± 8.7	.367
JSSF lesser scale (points)	75.0 ± 15.6	80.6 ± 11.1	63.0 ± 17.5	< .001
HV angle before operation (°)	41.4 ± 16.4	41.1 ± 17.9	42.1 ± 12.3	.757
HV angle at final follow-up (°)	19.2 ± 11.7	17.9 ± 12.1	22.2 ± 10.3	.077
Resection arthroplasty space immediately after K-wire removal (sum of all MTPJs) (mm)	16.6 ± 9.9	16.5 ± 9.4	16.9 ± 11.0	.838
Resection arthroplasty space at final follow-up visit (sum of all MTPJs) (mm)	6.3 ± 4.5	6.9 ± 4.6	5.0 ± 3.9	.042
Size of osteophytes (mm)	12.3 ± 7.1	11.9 ± 7.1	13.0 ± 7.1	.485
Hammer toe recurrence (n[†])	49 (46)	30 (41)	19 (58)	.018

Abbreviations: HV, hallux valgus; JSSF lesser scale, Japanese Society for Surgery of the Foot lesser metatarsophalangeal-interphalangeal scale; MTPJ, metatarsophalangeal joint.
Data presented as mean ± standard deviation or n (%).
* $p < .001$ vs preoperative values.
† Of total 428 toes (rays) included in the present study.

toes were more than twice as likely to have an unsatisfactory result (odds ratio [OR] 2.66, 95% CI 1.07 to 6.97, $p = .035$). The residual joint space in the resected joint at the final follow-up visit was negatively related to unsatisfactory results (OR 0.85 for a 1-unit increase, 95% CI 0.74 to 0.96; $p = .008$). The hallux valgus angle at the final follow-up visit was also a risk factor for an unsatisfactory result (OR 1.04 for a 1-unit increase, 95% CI 1.00 to 1.09; $p = .041$). The disease duration (OR 1.00 for a 1-unit increase, 95% CI 0.95 to 1.06, $p = .964$), duration of the observation period (OR 0.99 for a 1-unit increase, 95% CI 0.97 to 1.00, $p = .069$), and the size of the osteophytes (OR = 1.03 for a 1-unit increase, 95% CI 0.96 to 1.10, $p = .440$) were not significantly related statistically to an unsatisfactory result.

Painful callosities developed in 23 of 107 feet (22%), with 3 callosities (2.8%) localized to the dorsum and 20 (19%) to the sole of the foot. All callosities on the sole developed plantar to either the second or third MTPJ, with the exception of 1 (.9%) under the first metatarsal head. Regarding the second and third rays, of the 151 toes without recurrent hammer toe deformity, only 5 (3%) developed painful callosities, but 14 of 63 toes (22%) with recurrent hammer toe deformity displayed painful callosities. This difference was statistically significant ($p < .001$; Table 5). The mean size of the osteophytes localized to the second and third metatarsal stumps was 3.2 ± 2.2 mm in the rays without callosities and 3.3 ± 2.2 mm in the toes with callosities; this difference was not statistically significant ($p = .410$).

Preoperatively, 97 of the 107 feet (90.7%) had more than 1 dislocated MTPJ localized to the lesser rays (Table 1). Of the 269 lesser rays with preoperative MTPJ dislocation, 83 (31%) displayed hammer toe recurrence, and 30 of 159 lesser toes (19%) without preoperative dislocation showed recurrence. This difference was statistically significant (p = .007; Table 6).

Discussion

Resection arthroplasty for RA forefoot deformities, pioneered by Hoffmann (5) in 1912, has been modified by various surgeons, with good results (6,7,8,9,10,11,12,13). In our study, 69% of patients subjectively rated their surgical outcome as either excellent or good, with a mean follow-up of 5.8 ± 3.1 years. This incidence of postoperative satisfaction was comparable to that of previous reports with a similar follow-up period and procedure (11,26,33). Previous studies have shown unsatisfactory results after panmetatarsal head excision to be associated with several risk factors, including the recurrence of hallux valgus (26,27,28), hammer toe deformity, painful callosities (29), uneven and insufficient bone resection (34), and bone proliferation at the stump of the metatarsal (7,12). In our study, the major reasons for postoperative dissatisfaction were pain and the recurrence of toe deformity.

The recurrence of hammer toe deformity was more common in the unsatisfied patients than in the satisfied patients (58% vs 41%, $p = .0181$). Recurrent hammer toe deformities were also strongly related to the development of painful callus ($p < .001$), supporting the theory proposed by Brattstrom and Brattstrom (18) that hammer toe deformities formed in the postoperative course can lead to the development of callosities on the sole of the operated foot. Our multivariate regression analysis results showed that recurrent hammer toe deformity was 1 of the major risk factors for patient dissatisfaction (OR 2.66) after panmetatarsal head excision. Thus, avoidance of recurrent hammer toe deformity should be an important consideration for reducing the risk of patient dissatisfaction after this operation.

In the present study, we routinely resected all 5 metatarsal heads, including that of the first ray. The ideal management of the first metatarsal and hallux remains a divided issue, with some surgeons advocating resection (6,18,19,20), others arthrodesis (21,22,23), and still others silicone spacer arthroplasty (24,25). Arthrodesis of the first MTPJ provides stability to the ray but has several disadvantages, including a more demanding operative technique (35), degeneration of the interphalangeal joint (22), excessive pressure on the first toe (22), and relatively high complication and reoperation rates (36). We believe that silicone implant arthroplasty of the first MTPJ is rarely indicated because of the risk of fracture, infection, silicone synovitis, and osteolysis associated with the procedure (14,25). The most common criticism regarding the use of resection of the first metatarsal head has been the high rate of recurrence of hallux valgus

Table 4
Multivariate logistic regression analysis results depicting associations of risk factors with unsatisfactory result (n = 35 feet in 20 patients)

Risk Factor	OR	95% CI	*p* Value
Disease duration (y)	1.00	0.95 to 1.06	.964
Observation period (mo)	0.99	0.97 to 1.00	.069
Hallux valgus angle at final follow-up visit (°)	1.04	1.00 to 1.09	.041
Size of largest osteophyte (mm)	1.03	0.96 to 1.10	.440
Resection arthroplasty space at final follow-up visit (mm)	0.85	0.74 to 0.96	.008
Recurrence of hammer toe	2.66	1.07 to 6.97	.035

Abbreviations: CI, confidence interval; OR, odds ratio.
* Odds ratios for 1-unit increase in each item.

Table 5
Relationship between recurrence of hammer toe deformity and painful keratoma localized to second and third toes (n = 214 toes in 64 patients)

Painful Keratoma*	Recurrence of Hammer Toe (second and/or third toe)		Row Total	*p* Value
	Yes	No		
Yes	14	5	19	< .001
No	49	146	195	

* Digital keratoma localized to second and/or third toe postoperatively.

Table 6
Relationship between recurrence of hammer toe deformity and preoperative MTPJ dislocation (n = 428 toes in 64 patients)

Preoperative MTPJ Dislocation	Hammer Toe Recurrence		Row Total	*p* Value
	Yes	No		
Yes	83	186	269	.007
No	30	129	159	

Abbreviation: MTPJ, metatarsophalangeal joint.

deformity (26,27,28). In our study, the hallux valgus angle at the final follow-up visit was identified as a risk factor for unsatisfactory results; however, the OR was only 1.04. The average hallux valgus angle was 19.1° after more than 5 years of follow-up, significantly smaller than the preoperative angle of 41.4° ($p < .001$). Resection of the first metatarsal head, which we have recommended, could lead to recurrence of hallux valgus (11,26,33); however, its effect on our patients' satisfaction seemed to be limited.

Our observations also indicated that the amount of excessive bone formation at the second and third metatarsal stumps was rather high, and this result was consistent with the report by Vahvanen et al (26) that noted 72% of 179 operated feet with 1 or more metatarsal stumps displaying bony proliferations at the 5-year follow-up visit. They also reported that the bony proliferations were most commonly localized to the second and third metatarsal stumps (26). Heterotopic bone formation at the metatarsal stump has been cited as a factor for the development of painful callosities on the soles during the postoperative course (7,12). In contrast, Coughlin (13) reported that heterotopic bone formation occurred in 16 of the 188 lesser toes (9%) and that only 2 of these were associated with a plantar keratotic lesion. Our study showed no significant difference in the size of osteophytes at the stump between those with and without painful callosities, and the size of the osteophytes was not detected as a risk factor for patient dissatisfaction.

Insufficient bone resection has been thought to cause bony prominences at the metatarsal stumps or the recurrence of painful callosities (34), which has generally been associated with patient dissatisfaction. In our series, the residual joint space in the resected joint at the final follow-up visit was negatively related to unsatisfactory results (OR 0.85), and the length of the excision space immediately after surgery was not related to patient satisfaction. Patsalis et al (37) indicated diminution of the arthroplasty space as the most striking feature in those with unsatisfactory results and observed extensor tendon tightness with clawing of the toes in such cases. Combined with our finding that preoperatively dislocated lesser toes were more likely to have recurrent hammer toe deformities (31%) than those without dislocation (19%), we believe that the management of the soft tissue structures should be a more important consideration when treating these patients, rather than the amount of resection. Resection of the proximal phalanx base also has the potential to be related to recurrent deformity because of the subsequent destabilization. We could not address this issue adequately in our study, because we had only 1 case of proximal phalanx base excision and that patient belonged to the satisfactory group.

One of the limitations of the present study was our use of the Likert scale for measuring the patient satisfaction levels, because it yields ordinal rather than interval data. However, the JSSF lesser scale score was significantly different between the satisfactory and unsatisfactory groups, indicating good reliability for these groups. Another limitation was that the present study included some cases with relatively short follow-up periods (just >1 year). A minimum of 5 years would have more accurately reflected a midterm result of the procedures. We also appreciated that certain selection biases could have been present related to potential participant inclusion (diagnosis and procedure coding), recall issues, and that the treating surgeons also participated in procurement of the results used in the analyses.

In conclusion, the results of 107 forefoot arthroplasties in 64 patients followed up for a period of 5.8 ± 3.1 years were reviewed and analyzed. The observed incidence of postoperative patient satisfaction was 69%, which appears to be comparable to existing reports of forefoot arthroplasties with panmetatarsal head resection. The multivariate regression analyses showed that a decreased residual joint space at the final follow-up visit and recurrence of hammer toe deformities were major risk factors for patient dissatisfaction but that the recurrence of hallux valgus and the production of osteophytes had little effect on patient dissatisfaction. Our patients' unbiased and subjective assessment of their overall satisfaction showed they were subjectively more concerned with deformity of the lesser toes than that of the great toe. This finding suggests that better results might be achieved by taking care to sufficiently release the MTPJ contracture, especially in the case of dislocated MTPJs. Also, this could be an interesting area for future patient-oriented investigations.

References

1. Wickman AM, Pinzur MS, Kadanoff R, Juknelis D. Health-related quality of life for patients with rheumatoid arthritis foot involvement. Foot Ankle Int 25:19–26, 2004.
2. Michelson J, Easley M, Wigley FM, Hellmann D. Foot and ankle problems in rheumatoid arthritis. Foot Ankle Int 15:608–613, 1994.
3. Turner DE, Helliwell PS, Siegel KL, Woodburn J. Biomechanics of the foot in rheumatoid arthritis: identifying abnormal function and the factors associated with localised disease "impact.". Clin Biomech (Bristol, Avon) 23:93–100, 2008.
4. Baan H, Drossaers-Bakker W, Dubbeldam R, van de Laar M. We should not forget the foot: relations between signs and symptoms, damage, and function in rheumatoid arthritis. Clin Rheumatol 30:1475–1479, 2011.
5. Hoffmann P. An operation for severe grades of contracted or clawed toes. Am J Orthop Surg 9:441–449, 1912.
6. Fowler AW. A method of forefoot reconstruction. J Bone Joint Surg Br 41-B:507–513, 1959.
7. Clayton ML. Surgery of the forefoot in rheumatoid arthritis. Clin Orthop 16:136–140, 1960.
8. Kates A, Kessel L, Kay A. Arthroplasty of the forefoot. J Bone Joint Surg Br 49:552–557, 1967.
9. Faithful DK, Savill DL. Review of the results of excision of the metatarsal heads in patients with rheumatoid arthritis. Ann Rheum Dis 30:201–202, 1971.
10. Barton NJ. Arthroplasty of the forefoot in rheumatoid arthritis. J Bone Joint Surg Br 55:126–133, 1973.
11. Goldie I, Bremell T, Althoff B, Irstam L. Metatarsal head resection in the treatment of the rheumatoid forefoot. Scand J Rheumatol 12:106–112, 1983.
12. Mann RA, Schakel ME II. Surgical correction of rheumatoid forefoot deformities. Foot Ankle Int 16:1–6, 1995.
13. Coughlin MJ. Rheumatoid forefoot reconstruction: a long-term follow-up study. J Bone Joint Surg Am 82:322–341, 2000.
14. Hanyu T, Yamazaki H, Murasawa A, Tohyama C. Arthroplasty for rheumatoid forefoot deformities by a shortening oblique osteotomy. Clin Orthop Relat Res 338:131–138, 1997.
15. Takakubo Y, Takagi M, Tamaki Y, Sasaki A, Nakano H, Orui H, Ogino T. Mid-term results of joint-preserving procedures by a modified Mann method for big toe deformities in rheumatoid patients undergoing forefoot surgeries. Mod Rheumatol 20:147–153, 2010.
16. Krause FG, Fehlbaum O, Huebschle LM, Weber M. Preservation of lesser metatarsophalangeal joints in rheumatoid forefoot reconstruction. Foot Ankle Int 32:131–140, 2011.
17. Niki H, Hirano T, Okada H, Beppu M. Combination joint-preserving surgery for forefoot deformity in patients with rheumatoid arthritis. J Bone Joint Surg Br 92:380–386, 2010.
18. Brattstrom H, Brattstrom M. Resection of the metatarsophalangeal joints in rheumatoid arthritis. Acta Orthop Scand 41:213–224, 1970.
19. Clayton ML, Leidholt JD, Clark W. Arthroplasty of rheumatoid metatarsophalangeal joints: an outcome study. Clin Orthop Relat Res 340:48–57, 1997.
20. Grondal L, Brostrom E, Wretenberg P, Stark A. Arthrodesis versus Mayo resection: the management of the first metatarsophalangeal joint in reconstruction of the rheumatoid forefoot. J Bone Joint Surg Br 88:914–919, 2006.
21. Mann RA, Thompson FM. Arthrodesis of the first metatarsophalangeal joint for hallux valgus in rheumatoid arthritis. J Bone Joint Surg Am 66:687–692, 1984.
22. Beauchamp CG, Kirby T, Rudge SR, Worthington BS, Nelson J. Fusion of the first metatarsophalangeal joint in forefoot arthroplasty. Clin Orthop Relat Res 190:249–253, 1984.
23. Rosenbaum D, Timte B, Schmiegel A, Miehlke RK, Hilker A. First ray resection arthroplasty versus arthrodesis in the treatment of the rheumatoid foot. Foot Ankle Int 32:589–594, 2011.